Supplementary Information (SI) for Journal of Materials Chemistry C.
This journal is © The Royal Society of Chemistry 2025

Engineering of Imidazo[1,2-a]pyridine into Multifunctional Dual-State Emissive (DSE) Luminogens for Hydrazine Sensing and Cell-imaging

*Gauravi Yashwantrao,[a] Prajakta Gosavi,[a] Vaishnavi Naik,[b] Monalisha Debnath,[c] Saona Seth,[d] Purav Badani,[b] Rohit Srivastava,[c] and Satyajit Saha[a]**

[a]Department of Speciality Chemicals Technology, Institute of Chemical Technology (ICT), Mumbai, Maharashtra-400019, India

[b]Department of Chemistry, University of Mumbai, Kalina Campus, Mumbai, Maharashtra, India

[c]Department of Biosciences and Bioengineering, Indian Institute of Technology Bombay, Mumbai, Maharashtra, India

[d]Department of Applied Sciences, Tezpur University, Assam, India

Corresponding author e-mail: ss.saha@ictmumbai.edu.in

Table of Contents

General aspects

All chemicals were purchased from available commercial sources like Sigma-Aldrich, Spectrochem, and S. D. Fine chemicals and used without further purification. Organic solvents were dried and distilled before use. Silica gel-coated aluminium sheets (ACME, 254F) were used for the Thin Layer Chromatography (TLC) analysis using EtOAc and petroleum ether as the eluents to monitor the reaction progress. Melting points of all the compounds were recorded by the AnalabThermoCal melting point apparatus in the open capillary tube. Fourier transform infrared (FTIR) (ATR-IR) spectra were obtained with Alpha-II/Bruker-instrument. The ^{1}H Nuclear Magnetic Resonance (^{1}H NMR) spectroscopy was carried out on Bruker 400 spectrometer whereas 13C NMR was carried out on 100 MHz spectrometer using $CDCl_3$ as a solvent. Chemical shifts are reported in parts per million (ppm) downfield from TMS, and the spin multiplicities are described as s (singlet), d (doublet), t (triplet), and multiplet (m). Coupling constant (J) values are reported in hertz (Hz). Thermogravimetric analysis (TGA) was conducted on a Perkin-Elmer Diamond TG/DTA instrument at a heating rate of 10 °C/min under a nitrogen atmosphere with a flow rate of 150 mL/min. UV-Visible absorption spectra were obtained on a FP-8200/Jasco spectrophotometer. Cyclic voltammetry (CV) measurements were measured in an electrolyte solution of tetrabutylammonium hexafluorophosphate ($^{t}Bu_4NPF_6$) in DMF (0.1 M), using platinum gauze and Ag/AgCl as the counter and reference electrodes respectively. A scan rate of 25 mV/s was used during the CV measurements.

Photophysical Properties of GBY-12, GBY-13, GBY-14 and GBY-15

Preparation of stock solution luminogens in THF solvent

Here, for **GBY-12**
Molecular weight = 553.22 g
Therefore, 553.22 g in 1000 mL of THF ≡ 1M

$$Concentration\ (M) = \frac{Mass\ (g)}{Formula\ weight\ (g) * Volume\ (L)}$$

Hence, to prepare 1mM stock solution 5.53 mg of **GBY-12** was dissolved in 10ml THF
Similarly, stock solution for **GBY-13, GBY-14 and GBY-15** and **L3** was prepared.

Solvatochromic property:

For UV-Visible absorption studies, the UV-visible absorption measurement was performed in a JASCO V-750 spectrophotometer under room temperature using two side opaque and two side transparent quartz cuvettes having path length equalled to 1 cm. For solution state measurement, concentration of the luminogens **GBY-12, GBY-13, GBY-14 and GBY-15** stock was kept at 1 mM. For photoluminescence studies, the emission measurement was performed in a JASCO FP-8200 spectrofluorimeter under room temperature using all side transparent quartz cuvette with path length equal to 1cm. Likewise absorption studies, concentration of the luminogen was kept at 1 mM throughout the solution state measurement.

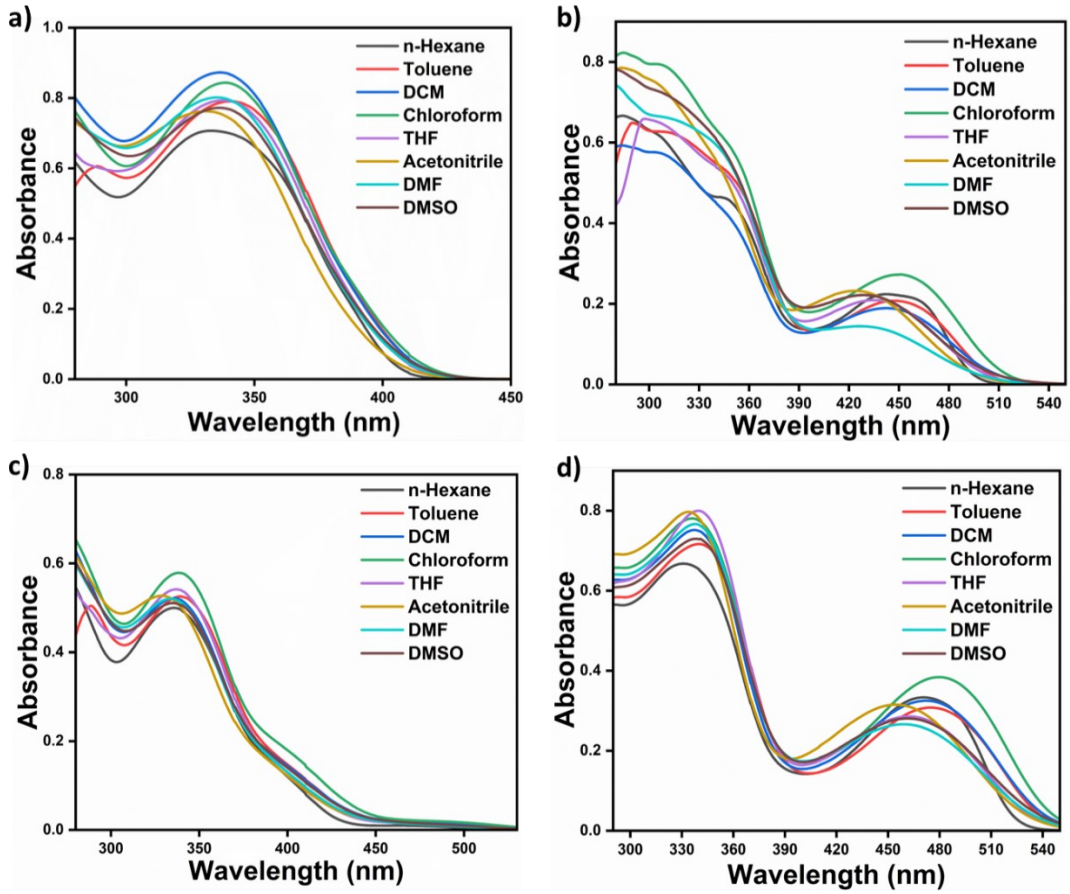

Figure S1. Solvatochromic properties of **GBY-12, GBY-13, GBY-14 and GBY-15.**

Table S1. Stoke's shift for calculation for **GBY-12**

GBY-12				
Solvent	λabs	λemi	Stokes shift	
			(nm)	(cm^{-1})
n-Hexane	333	500.5	167.5	10050.01
Toluene	341	461	120	7633.539
DCM	336.5	491.5	155	9371.802
Chloroform	338.5	495.5	157	9360.463
THF	337.5	481.5	144	8861.198
Acetonitrile	331	503	172	10330.76
DMF	335.5	493.5	158	9542.835
DMSO	336.5	504.5	168	9896.076

Table S2. Stoke's shift calculation for **GBY-13**

GBY-13				
Solvent	λabs (nm)	λemi (nm)	Stokes shift	
			(nm)	(cm^{-1})
n-Hexane	442.5	506	63.5	-63.5
Toluene	447	543.5	96.5	-96.5
DCM	442.5	566	123.5	-123.5
Chloroform	450.5	561	110.5	-110.5
THF	435	563.5	128.5	-128.5
Acetonitrile	423.5	562	138.5	-138.5
DMF	390	567	177	-177
DMSO	429	570	141	-141

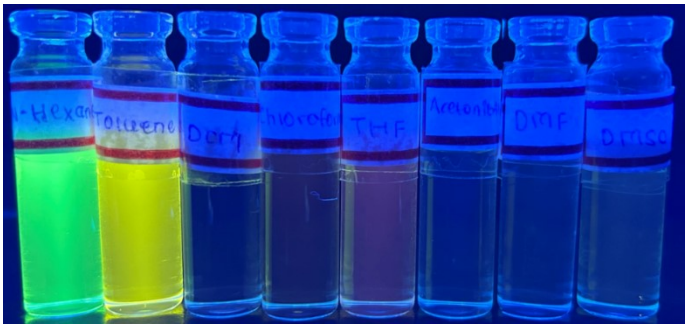

Figure S2. Effect of different solvent polarity on **GBY-13** visualized under UV light (365 nm).

Table S3. Stoke's shift calculation for **GBY-14**

GBY-14				
Solvent	λabs	λemi	Stokes shift	
			(nm)	(cm^{-1})
n-Hexane	336	465	129	8256.528
Toluene	339.5	477.5	138	8512.673
DCM	337	482	145	8926.703
Chloroform	335.5	493	157.5	9522.284
THF	338.5	494	155.5	9299.183
Acetonitrile	329	498	169	10314.82
DMF	334	496	162	9778.829
DMSO	335	502	167	9930.428

Figure S3. Effect of different solvent polarity on **GBY-14** visualized under UV light (365 nm).

Table S4. Stoke's shift calculation for **GBY-15**

GBY-15				
Solvent	**λabs (nm)**	**λemi (nm)**	**Stokes shift**	
			(nm)	**(cm^{-1})**
n-Hexane	331	527.5	196.5	11254.13
	470.5		57	2296.639
Toluene	340	554.5	214.5	11377.5
	475		79.5	3018.366
DCM	337	565	228	11974.48
	472		93	3487.326
Chloroform	336	564.5	228.5	12047.11
	479.5		85	3140.266
THF	340.5	566	225.5	11700.73
	462		104	3977.177
Acetonitrile	334	572.5	238.5	12472.87
	454.5		118	4534.951
DMF	338	577	239	12254.78
	459		118	4455.47
DMSO	338	583.5	245.5	12447.84
	461.5		122	4530.512

Figure S4. Effect of different solvent polarity on **GBY-15** visualized under UV light (365 nm).

Aggregation induced emission

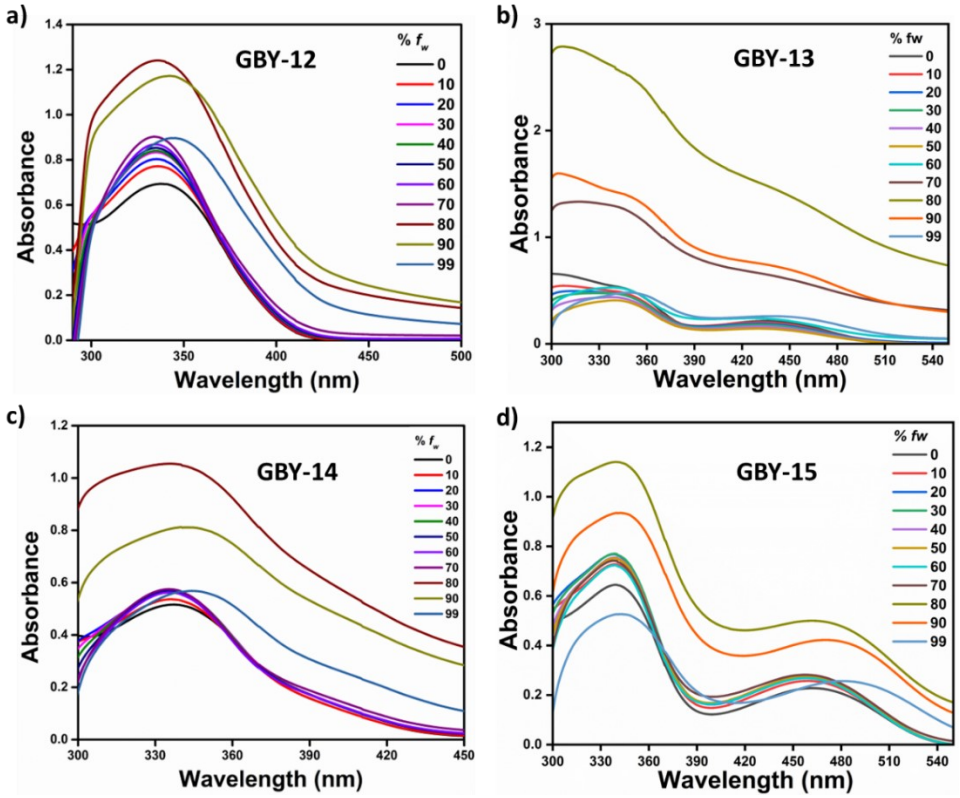

Figure S5. Absorption spectra of **GBY-12, GBY-13, GBY-14 and GBY-15** with incremental rise in H_2O fraction.

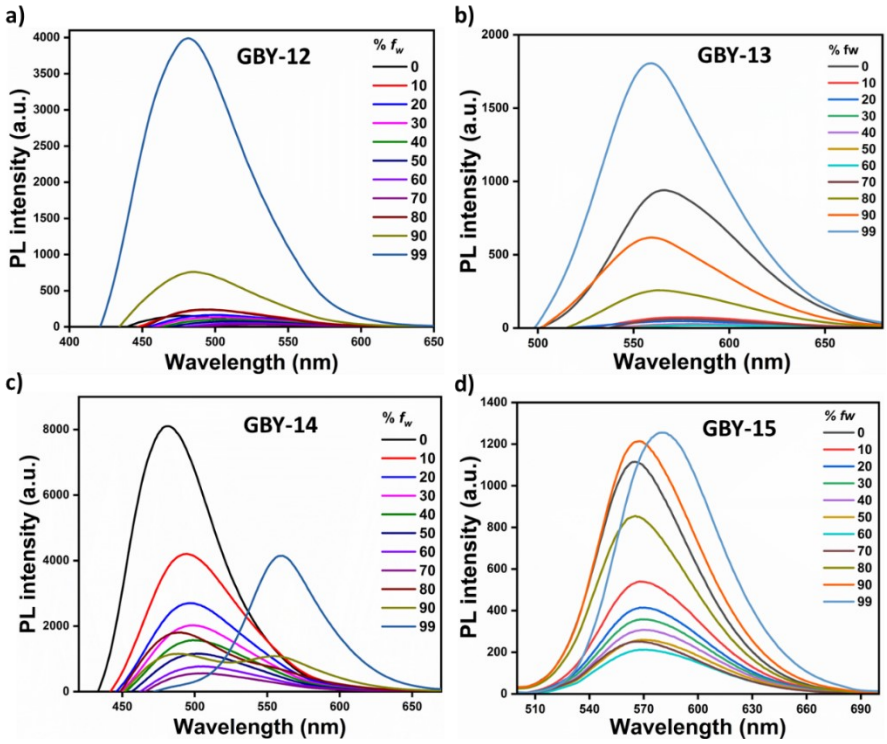

Figure S6. Emission spectra of **GBY-12, GBY-13, GBY-14 and GBY-15** with incremental rise in H_2O fraction at excitation wavelength 337.5 nm, 435 nm, 337 nm, and 462 nm respectively.

Tyndall Effect: The enhancement in emission intensity was attributed to the formation of aggregates, which was further validated by the Tyndall effect and DLS experiments. When a beam of light passes through a colloid, the colloidal particles present in the solution do not allow the beam to completely pass through. The light collides with the colloidal particles and is scattered (it deviates from its normal trajectory, which is a straight line). This scattering makes the path of the light beam visible. Tyndall effect [1] was observed when laser light was passed through the aggregated states (99% water) of luminogens.

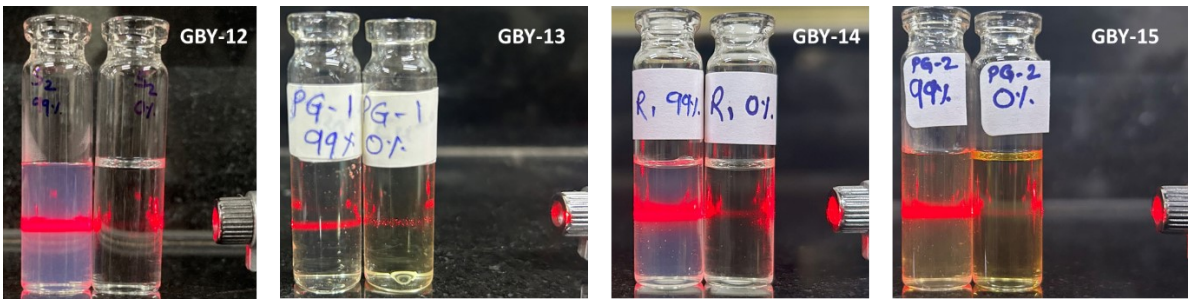

Figure S7. Observance of Tyndall effect on the aggregated states of **GBY-12, GBY-13, GBY-14, GBY-15**.

Dynamic light scattering (DLS) experiments: The size distribution of the evolved aggregates in THF at higher water fraction was determined through DLS experiment, using Malvern Zetasizer Nano-ZS90 instrument. A transparent disposable polystyrene cuvette with a path length equalled to 1 cm, containing the desired solution was utilized in the experiment. A 632.8 nm red laser was employed as an excitation source at a fixed scattering angle (90˚ optics)

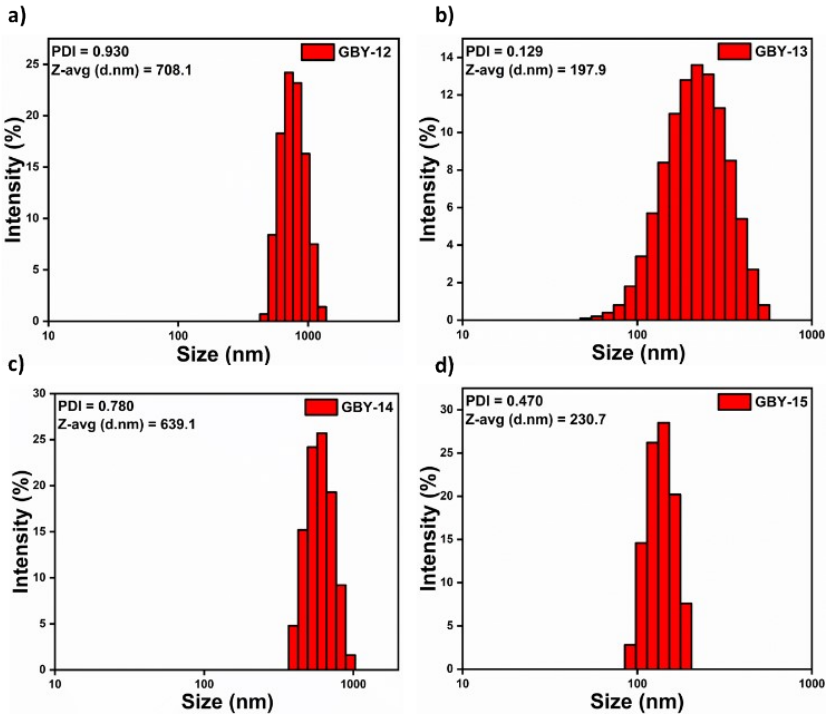

Figure S8. Particle size distribution profiles of the aggregated forms of **GBY-12, GBY-13, GBY-14, GBY-15** at fw 99%

Table S5. DLS parameter of luminogens **GBY-12, GBY-13, GBY-14** and **GBY-15** in THF at water fraction (99%).

Luminogens	Z-Average (nm)	PDI	Peak 1 (Size in nm)	Peak 1 (St.Dev in nm)
GBY-12	708.1	0.930	277.3	34.19
GBY-13	197.9	0.129	231.2	92.06
GBY-14	639.1	0.780	272.2	45.47
GBY-15	230.7	0.470	136.9	32.84

Scanning Electron Microscopy: Scanning electron microscope (SEM) images of luminogens **GBY-12, GBY-13, GBY-14** and **GBY-15** aggregates, were recorded using SEM Quanta 200 – EDX system. Before recording the images, sonicate the sample and was placed using glass capillary on the aluminium stub. Mount sample over carbon tape whose half portion was covered with aluminium foil on aluminium stub.

Preparation of Nanoaggregates: Nanoaggregates of luminogens **GBY-12, GBY-13, GBY-14** and **GBY-15** were prepared by adding 50 µL of stock solution (0.1 mM) in a solution containing 4.95 mL of water and 0.05 mL of THF with vigorous shaking.

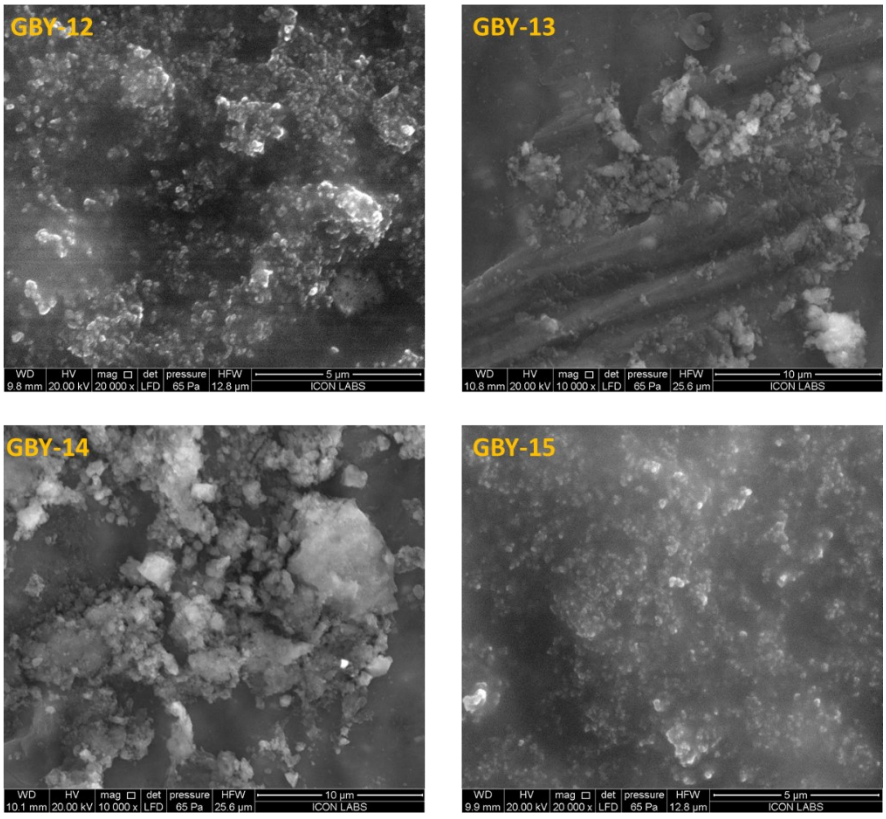

Figure S9. SEM images of the aggregate states **GBY-12, GBY-13, GBY-14** and **GBY-15.**

Detection of Trace Water

Limit of detection

Detection limit calculations for **GBY-13** (1 mM) in THF

σ = Standard Deviation obtained from 10 blank emission measurement of THF:Water (100:0.0 v/v)

σ = 3.2213

and k is slope obtained from Plot of emission intensity of **GBY-13** in THF:Water (100:0.0 v/v) at 435 nm versus water fraction (%)

k = 336.6708

Detection limit = 3σ/k

Detection limit = 3*3.2213/336.6708

Detection limit = 0.028 vol% (280 ppm)

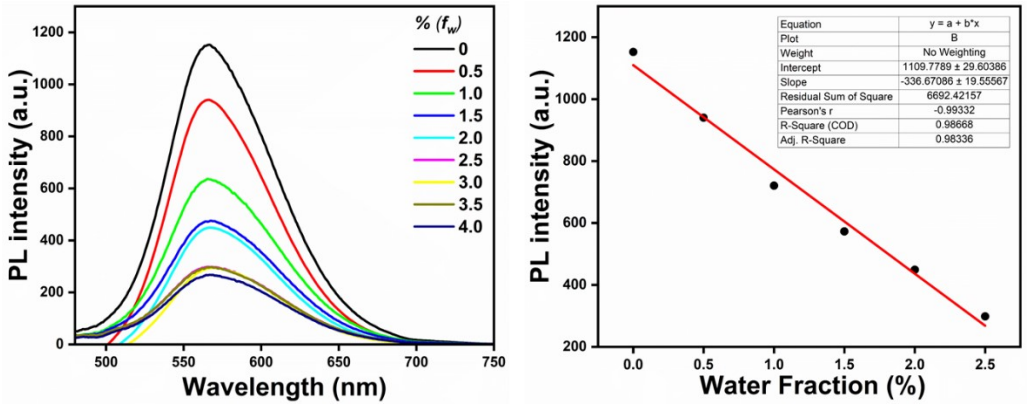

Figure S10. Moisture Sensing with **GBY-13** and Plot of water fraction (%) vs PL intensity.

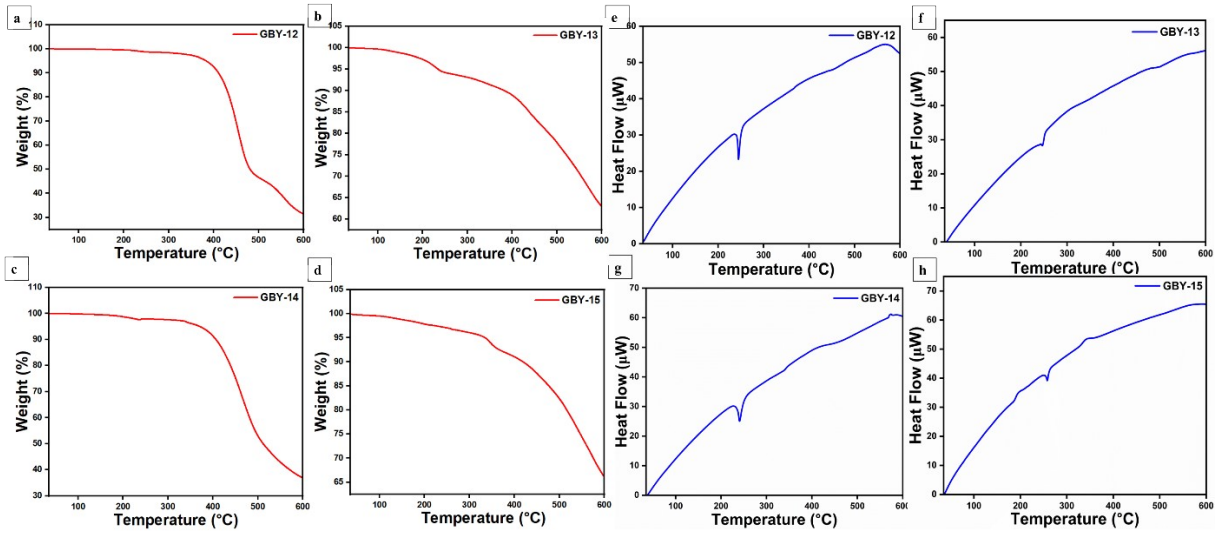

Figure S11. TGA-DSC profiles of the luminogens **GBY-12**, **GBY-13**, **GBY-14**, and **GBY-15**.

Cyclic Voltammetry Analysis of GBY-12, GBY-13, GBY-14 and **GBY-15:**

The electrochemical study was carried out by cyclic voltammetry. Cyclic voltammetry measurements were recorded in an electrolyte solution of 0.1 M tetrabutylammonium hexafluorophosphate (^{t}Bu$_4$NPF$_6$) in DMF using Ag/AgCl as reference electrode and platinum

gauze as the counter electrode. Glassy carbon electrode was used as a working electrode and the analysis was carried out at a scan rate of 25 mV/s. The concentration of all three analyte (Luminogens) used was 1 mM. To perform the experiment, the three-electrode system was subjected to a solution containing both analyte and electrolyte in 1:1 proportion.

HOMO and LUMO energies and HOMO-LUMO energy gap (EHL) of Luminogens **GBY-12, GBY-13, GBY-14 and GBY-15** calculated from experimental data as follows,

For **GBY-12**

Onset absorption wavelength (λmax) DMF: 338 nm

Onset CV oxidation: 1.12 V

E_{HOMO} = - (4.8 + $E_{OX\ onset}$) eV

= - (4.8 + 1.12) eV

= - 5.92 eV

$E_{band\ gap}$ = 1240/λ_{max}

= 1240/ 338

= 3.66 eV

E_{LUMO} = E_{HOMO} + $E_{band\ gap}$

= -5.92 + 3.66

= -2.26

For **GBY-13**

Onset absorption wavelength (λmax) DMF: 432 nm

Onset CV oxidation: 1.42 V

E_{HOMO} = - (4.8 + $E_{OX\ onset}$) eV

= - (4.8 + 1.42) eV

= - 6.22 eV

$E_{band\ gap}$ = 1240/λ_{max}

= 1240/ 432

= 2.87 eV

E_{LUMO} = E_{HOMO} + $E_{band\ gap}$

= -6.22 + 2.87

= -3.35 eV

For **GBY-14**

Onset absorption wavelength (λmax) DMF: 334.5 nm

Onset CV oxidation: 1.13 V

E_{HOMO} = - (4.8 + $E_{OX\ onset}$) eV

= - (4.8 + 1.13) eV

= - 5.93 eV

$E_{band\ gap}$ = 1240/λ_{max}

= 1240/ 334.5

= 3.70 eV

E_{LUMO} = E_{HOMO} + $E_{band\ gap}$

= -5.93 + 3.70

= -2.23 eV

For **GBY-15**
Onset absorption wavelength (λmax) DMF: 460, 337 nm
Onset CV oxidation: 1.36 V
E_{HOMO} = - (4.8 + $E_{OX\ onset}$) eV
= - (4.8 + 1.36) eV
= - 6.16 eV
$E_{band\ gap}$ = 1240/λ_{max}
= 1240/ 460
= 2.69 eV
E_{LUMO} = E_{HOMO} + $E_{band\ gap}$
= -6.16 + 2.69
= -3.47 eV

Table S6. Electrochemical Data of **GBY-12, GBY-13, GBY-14** and **GBY-15** in DMF.

Luminogens	E (Onset/ox) [V]	λ_{onset} (nm)	HOMO [eV]	LUMO [eV]	Band gap [eV]
GBY-12	1.12	338	-5.92	-2.26	3.66
GBY-13	1.42	432	-6.22	-3.35	2.87
GBY-14	1.13	334.5	-5.93	-2.23	3.70
GBY-15	1.36	460	-6.16	-3.47	2.69

E_{HOMO} = − (4.8 + Eox onset) eV
E_{LUMO} = E_{HOMO} + $E_{band\ gap}$
Band gap = (E LUMO – E HOMO) eV or 1240/ $\lambda_{max\ onset}$

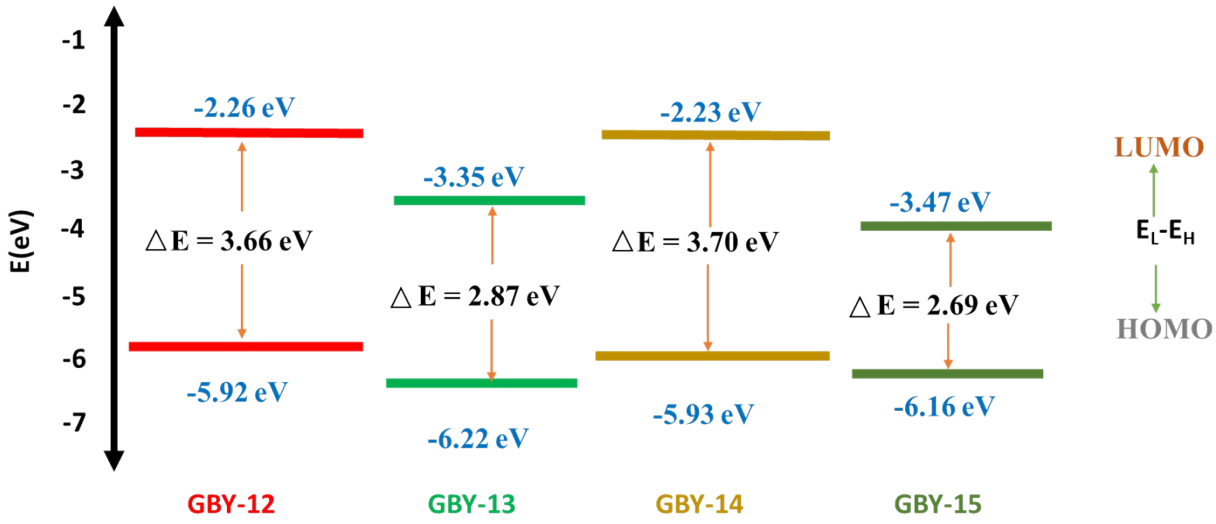

Figure S12. The experimentally calculated HOMO-LUMO energy gap of Luminogens **GBY-12, GBY-13, GBY-14** and **GBY-15** from cyclic voltammetry analysis

DFT Calculations

To evaluate the theoretical bandgap of the luminogens **GBY-12, GBY-13, GBY-14** and **GBY-15** density functional theory (DFT) calculations were performed at DFT/ B3LYP level of theory using the Gaussian 09 suite of program. Energy minimization of structures was carried out at a 6-311+G(d,p) basis.[2]

The DFT calculation results disclosed that for all the three luminogens **GBY-12, GBY-13, GBY-14** and **GBY-15**, the electron distribution of the HOMO is localised on entire moiety. However, in LUMO for **GBY-12, GBY-13, GBY-14** and **GBY-15**, the electrons have localized on heterocyclic moiety that is imidazopyridine core and electron withdrawing moieties.

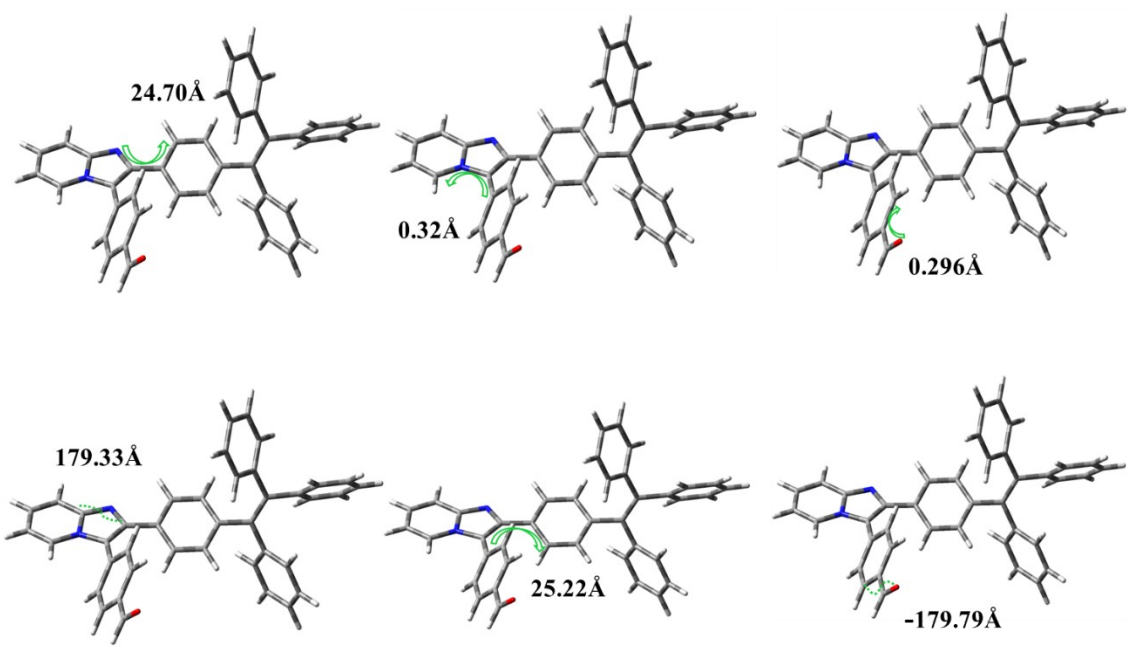

Figure S13. Dihedral angle existing in **GBY-12**

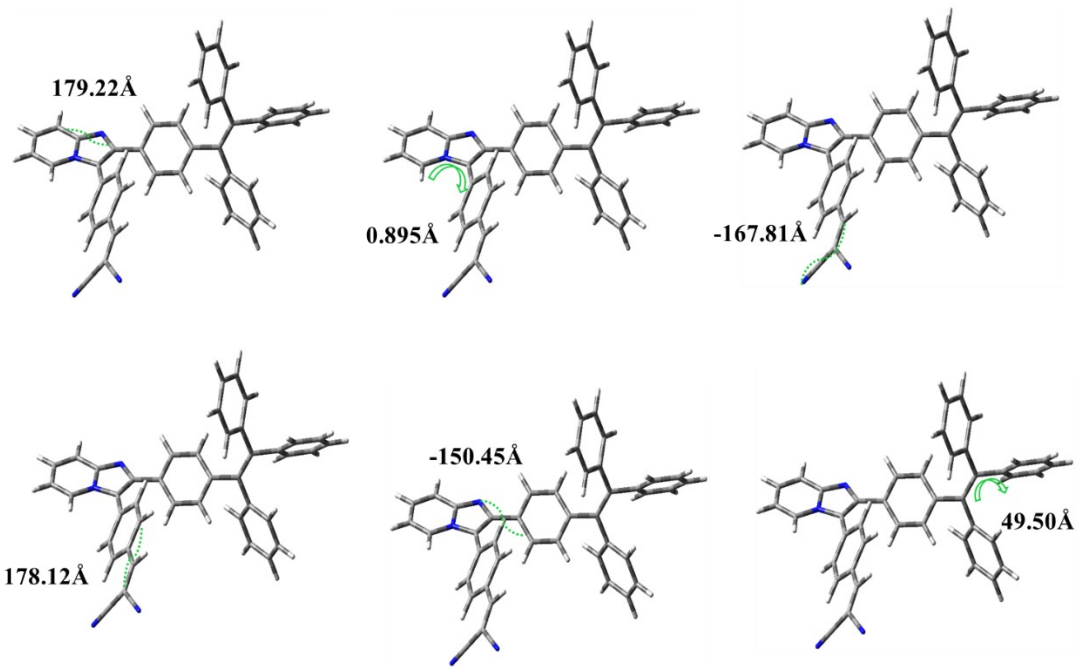

Figure S14. Dihedral angle existing in **GBY-13.**

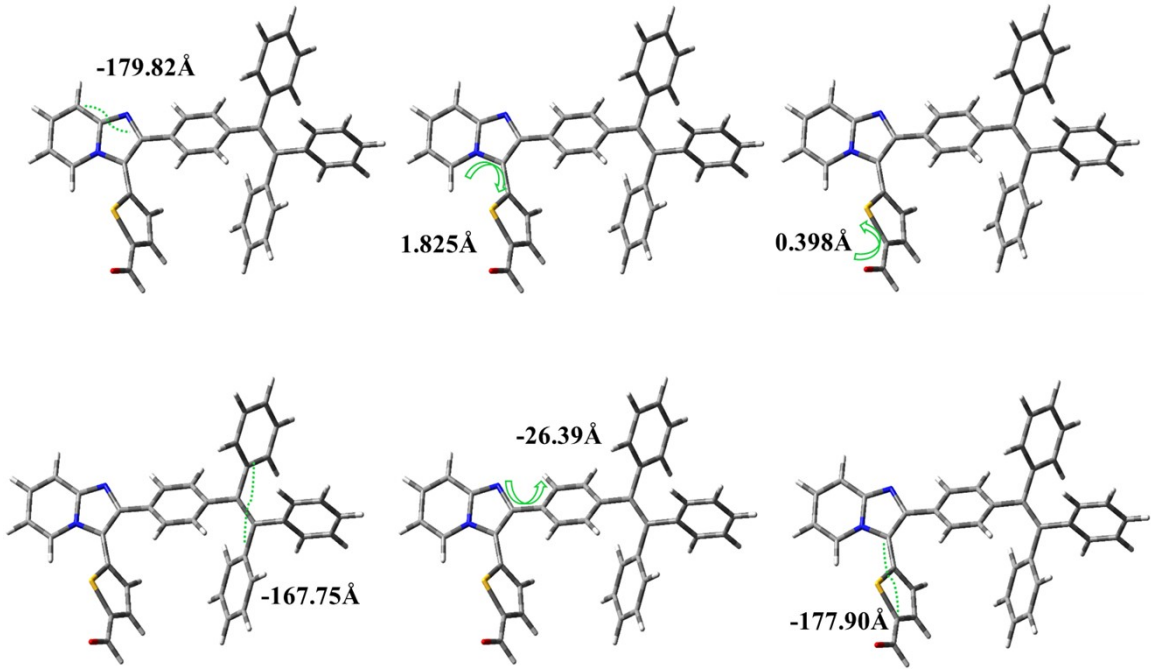

Figure S15. Dihedral angle existing in **GBY-14.**

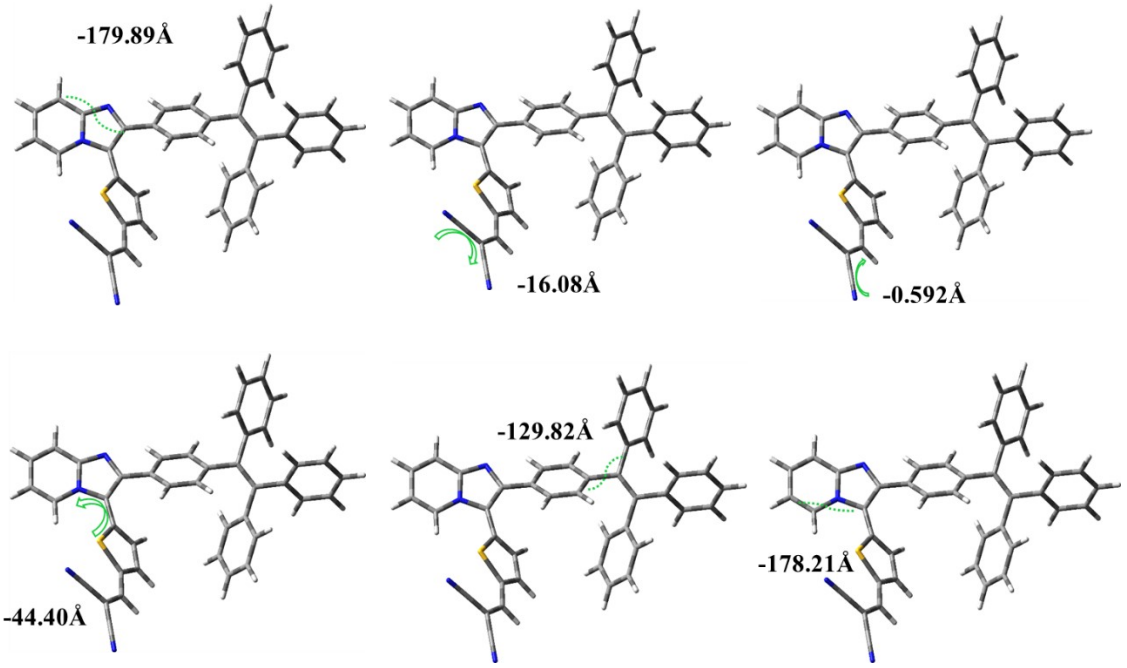

Figure S16. Dihedral angle existing in **GBY-15.**

In our current study, we focused on the geometry optimization of a given structures using the Gaussian 09 program. To achieve this, we employed the Density Functional Theory (DFT) approach, specifically utilizing the B3LYP functional and the 6-311G basis set. Furthermore, in order to refine the energy, we performed single-point energy calculations at the B3LYP/6-311++G (df,pd) level of theory. In addition to optimizing the structures and refining the energy calculations, we also investigated the impact of the solvent on the structures. To achieve this, we conducted single-point electronic structure calculations using an implicit CPCM model at the B3LYP/6-311++G (df,pd) level of theory. Specifically, we considered the n,n-Dimethylformamide (DMF) solvent environment. The Cartesian coordinates for the optimized structures are provided.

Cartesian Coordinates

GBY-12

Total energy: -1725.78546537 a.u.

Charge: 0

Spin: Singlet

Dipole moment: 4.0399 Debye

Function/Basis set: B3LYP/6-311G

C	-7.46038200	1.74524600	-1.31500300

C	-7.58579800	0.40541600	-0.84305500
C	-6.47860800	-0.32686000	-0.51469100
N	-5.22661000	0.24302600	-0.65283800
C	-5.06833300	1.58307400	-1.09045300
C	-6.21953800	2.32547900	-1.43082700
C	-3.94392500	-0.24722200	-0.36221400
C	-3.07097800	0.81261500	-0.65276500
N	-3.77345000	1.92234600	-1.09143200
C	-1.60524900	0.86993300	-0.58250600
C	-0.97785000	2.12159800	-0.44244700
C	0.40746700	2.22283600	-0.37508000
C	1.22686800	1.08186900	-0.45764200
C	0.59767400	-0.16330700	-0.64000900
C	-0.78951100	-0.27053500	-0.69332100
C	2.71769900	1.18383500	-0.41810900
C	3.38374500	1.90556900	0.53286800
C	4.84381300	2.21951400	0.43450100
C	2.70942500	2.44004800	1.75772700
C	3.42598000	0.43090500	-1.50146100
C	2.89820500	3.77786800	2.15177400
C	2.28699500	4.27956500	3.30158400
C	1.49055000	3.44826800	4.09449100
C	1.31245000	2.11150300	3.72775600
C	1.91444600	1.61307400	2.57165100
C	5.69227000	2.02208900	1.54013600

C	7.05153700	2.32846200	1.46456900
C	7.58877200	2.85840200	0.28785300
C	6.75425100	3.07966900	-0.81117900
C	5.39714100	2.76308700	-0.73892100
C	3.01799700	0.55605800	-2.84253100
C	3.66066600	-0.15568100	-3.85635100
C	4.71245200	-1.02354800	-3.54844500
C	5.11443300	-1.17372600	-2.21844700
C	4.47864900	-0.45360200	-1.20610500
C	-3.72440800	-1.59143700	0.18705500
C	-4.23637500	-2.73707900	-0.45533400
C	-4.02996800	-4.00461400	0.08328300
C	-3.30477400	-4.16283300	1.27374800
C	-2.78614500	-3.02528000	1.91735200
C	-2.99511800	-1.76083200	1.38449900
C	-3.09252200	-5.50577500	1.83370100
O	-2.46920600	-5.74174000	2.88011500
H	-8.34879400	2.30312700	-1.57326100
H	-8.56116900	-0.04449000	-0.73533300
H	-6.51634400	-1.33579400	-0.13979800
H	-6.08133400	3.34025100	-1.77005900
H	-1.59659100	3.00558100	-0.39772100
H	0.86568400	3.19500400	-0.26105200
H	1.20349500	-1.05307200	-0.74548300
H	-1.23554100	-1.24243800	-0.84651500

H	3.52431700	4.42302300	1.55012600
H	2.43510600	5.31483100	3.57995200
H	1.02130900	3.83502400	4.98941500
H	0.70907300	1.45667300	4.34289700
H	1.77314500	0.57798000	2.29390900
H	5.28115300	1.62432400	2.45820500
H	7.68851500	2.15806000	2.32275700
H	8.64144300	3.10196700	0.23067300
H	7.15810600	3.50074000	-1.72262200
H	4.75790200	2.93704900	-1.59288400
H	2.19656200	1.21647700	-3.08613700
H	3.33899900	-0.03615900	-4.88276500
H	5.20747300	-1.57979700	-4.33348700
H	5.92021700	-1.85151200	-1.96864900
H	4.79526300	-0.57359600	-0.17958600
H	-4.76778200	-2.63153800	-1.39155800
H	-4.42112500	-4.87775300	-0.42550800
H	-2.23209900	-3.15940000	2.83607400
H	-2.60250600	-0.88832800	1.88683200
H	-3.53210900	-6.33581500	1.25647900

GBY-13

Total energy: -1874.32945590 a.u.

Charge: 0

Spin: Singlet

Dipole moment: 5.6079 Debye

Function/Basis set: B3LYP/6-311G

C	-7.04597100	-3.92655900	2.06544500
C	-7.47102300	-2.77981000	1.33332400
C	-6.55827400	-1.91791200	0.79084800
N	-5.20890700	-2.16282500	0.96757200
C	-4.75379300	-3.31240600	1.66101600
C	-5.70566800	-4.19086100	2.22037900
C	-4.06785000	-1.48960700	0.49831400
C	-2.97902900	-2.25702400	0.94760800
N	-3.41491900	-3.36487300	1.64968200
C	-1.53672600	-2.01717400	0.80835100
C	-0.65685800	-3.11410900	0.85395500
C	0.71716900	-2.93297100	0.74005100
C	1.27366000	-1.64923800	0.58913000
C	0.39319100	-0.55146000	0.58383600
C	-0.98412900	-0.72978100	0.68337900
C	2.75201900	-1.44303300	0.50999300
C	3.55583900	-2.17297900	-0.32081900
C	5.04885300	-2.16044300	-0.21809600
C	3.01033500	-3.04559200	-1.40769700
C	3.28537500	-0.37623900	1.41540600
C	3.46987400	-4.36669600	-1.56306400
C	2.98155100	-5.17978300	-2.58655600
C	2.03859300	-4.68236500	-3.49073000
C	1.58919100	-3.36536600	-3.36185400
C	2.06868600	-2.55627400	-2.33080300

C	5.84339800	-2.00069800	-1.36894600
C	7.23630900	-2.00735400	-1.28502900
C	7.86559300	-2.19382400	-0.05084700
C	7.08955800	-2.37459900	1.09735200
C	5.69677200	-2.35737600	1.01479700
C	2.90919400	-0.33531400	2.77098000
C	3.38879200	0.66495000	3.61772000
C	4.23939700	1.65748700	3.12229300
C	4.60497300	1.64109200	1.77355200
C	4.13370500	0.63465700	0.92941900
C	-4.14839600	-0.28318000	-0.32631100
C	-4.94783300	0.81911900	0.04857400
C	-5.03269200	1.95768900	-0.74170400
C	-4.31275900	2.04994800	-1.95484500
C	-3.50222400	0.94785400	-2.32017300
C	-3.42341000	-0.18983300	-1.53210600
C	-4.33065800	3.18421600	-2.85933900
C	-5.01821700	4.36696000	-2.82145300
C	-4.83377200	5.31980500	-3.87530000
N	-4.67725300	6.09002700	-4.73928300
C	-5.93707800	4.74714800	-1.79617700
N	-6.69291800	5.06838600	-0.96524300
H	-7.78497300	-4.59033200	2.49001300
H	-8.52297200	-2.58118300	1.19515900
H	-6.82747300	-1.04846100	0.21572900

H	-5.34051800	-5.05509000	2.75287100
H	-1.07098000	-4.10179000	0.99291300
H	1.37211800	-3.79181000	0.77578700
H	0.79536700	0.44995800	0.51140000
H	-1.62733600	0.13835400	0.69383100
H	4.20987700	-4.75343300	-0.87537000
H	3.33904800	-6.19681200	-2.68092900
H	1.66497400	-5.31016000	-4.28877300
H	0.87024100	-2.96737900	-4.06626400
H	1.71911300	-1.53758500	-2.23684200
H	5.36354300	-1.86824000	-2.32934500
H	7.82851400	-1.87132100	-2.18055900
H	8.94554400	-2.20482000	0.01399000
H	7.56732400	-2.53150900	2.05554400
H	5.10329500	-2.49790900	1.90704200
H	2.24227900	-1.09390700	3.15834200
H	3.09651800	0.67173600	4.65967600
H	4.60695600	2.43653400	3.77695900
H	5.25420100	2.41141200	1.37841200
H	4.42180700	0.62702600	-0.11237300
H	-5.48052200	0.79524900	0.98930500
H	-5.64715800	2.77567000	-0.40185800
H	-2.94039400	0.99166100	-3.24469000
H	-2.80667100	-1.02023900	-1.84310400
H	-3.68418900	3.07059500	-3.72245800

GBY-14

Total energy: -2046.53638541 a.u.

Charge: 0

Spin: Singlet

Dipole moment: 3.3665 Debye

Function/Basis set: B3LYP/6-311G

C	-7.23031900	1.04823900	-3.14852600
C	-7.51732900	0.69529200	-1.79871400
C	-6.52094700	0.63749400	-0.86306700
N	-5.22481100	0.93056000	-1.24063900
C	-4.90282100	1.26331100	-2.57811500
C	-5.93891000	1.32516700	-3.53243200
C	-4.01664700	0.92265600	-0.51949500
C	-3.02690900	1.27510300	-1.45835200
N	-3.58250200	1.46712700	-2.70589800
C	-1.58329800	1.46544000	-1.27241300
C	-1.01844100	1.86574100	-0.04852500
C	0.35739100	2.03059600	0.08103800
C	1.22334400	1.81176400	-1.00544000
C	0.64864900	1.46025700	-2.24141800
C	-0.72482700	1.28372300	-2.37247200
C	2.70000900	2.00195700	-0.87435800
C	3.42403400	1.44431600	0.14237300
C	4.84052700	1.82942600	0.43434400
C	2.86248100	0.39324700	1.04877800
C	3.32171900	2.84652900	-1.94243700

C	3.00732200	0.49942900	2.44468300
C	2.50895000	-0.48857400	3.29487600
C	1.87262800	-1.61593200	2.76664700
C	1.73923700	-1.74505000	1.38102400
C	2.22795100	-0.75084800	0.53182400
C	5.82105500	0.84130600	0.64245800
C	7.14021300	1.19056000	0.93386300
C	7.50383700	2.53589200	1.04337500
C	6.53635800	3.52765200	0.85987900
C	5.21954600	3.17839700	0.55764300
C	2.74177700	4.07580200	-2.30756800
C	3.30401700	4.86238800	-3.31375900
C	4.44724000	4.42736700	-3.99029000
C	5.02113900	3.19831500	-3.65352100
C	4.46472500	2.41666700	-2.64032200
C	-3.92096400	0.53392200	0.86640000
C	-3.02451900	-0.34450000	1.43542800
C	-3.13840600	-0.47845400	2.84198400
C	-4.13456400	0.28096800	3.41095800
S	-4.99214100	1.26936500	2.15879700
C	-4.52622300	0.33386200	4.79875600
O	-5.45388100	1.02505900	5.25671000
H	-8.03398900	1.09344400	-3.86904200
H	-8.52875600	0.46909400	-1.49750200
H	-6.68334300	0.37441200	0.16799900

H	-5.67568400	1.58790500	-4.54503000
H	-1.65558800	2.07011800	0.79931000
H	0.76852000	2.34279100	1.03058200
H	1.28862900	1.31998100	-3.10205800
H	-1.15676400	1.01241600	-3.32445700
H	3.51169900	1.36164500	2.85966400
H	2.62284100	-0.38210600	4.36581200
H	1.49875800	-2.38903600	3.42518300
H	1.26548600	-2.62293100	0.96088500
H	2.12526700	-0.85904200	-0.53877100
H	5.54451100	-0.20208600	0.57118000
H	7.88111500	0.41514300	1.07893100
H	8.52524900	2.80713800	1.27523700
H	6.80525500	4.57160100	0.95398100
H	4.47681000	3.95093100	0.41680500
H	1.84943900	4.41258300	-1.79730000
H	2.84845700	5.80939400	-3.57200500
H	4.88011600	5.03417600	-4.77452300
H	5.89859100	2.84691600	-4.18040700
H	4.91319400	1.46693400	-2.38520100
H	-2.29808200	-0.87965700	0.84382600
H	-2.50842200	-1.13389200	3.42676600
H	-3.92549100	-0.30510200	5.46596000

GBY-15

Total energy: -2195.08301479 a.u.

Charge: 0

Spin: Singlet

Dipole moment: 6.8750 Debye

Function/Basis set: B3LYP/6-311G

C	-7.02359000	-1.39575300	3.71326400
C	-7.43732600	-1.14500400	2.37497000
C	-6.51736100	-0.98886900	1.37399800
N	-5.17142200	-1.08111000	1.67331900
C	-4.72949400	-1.31025700	2.99738500
C	-5.68452700	-1.47328200	4.01970100
C	-4.01639700	-0.93558100	0.87732400
C	-2.93425700	-1.11693500	1.76893500
N	-3.38653200	-1.32947600	3.04962300
C	-1.49085500	-1.13407200	1.50203900
C	-0.94709600	-1.58105300	0.28471900
C	0.42879900	-1.58273900	0.07790800
C	1.31665100	-1.14836500	1.07857100
C	0.77062600	-0.75279700	2.31407300
C	-0.60477800	-0.73905500	2.52110100
C	2.79542300	-1.15994300	0.86164600
C	3.37499400	-0.60909000	-0.24730500
C	4.81009100	-0.83317500	-0.60712600
C	2.62245700	0.27315000	-1.19452600
C	3.58525400	-1.81717000	1.94977700
C	2.69682200	0.05952900	-2.58374900
C	2.01991700	0.89312300	-3.47499500
C	1.27075300	1.97291000	-2.99761500

C	1.20425900	2.20995700	-1.62134800
C	1.87123000	1.36795300	-0.72977700
C	5.63506200	0.25049400	-0.96217500
C	6.96938300	0.04910400	-1.31738900
C	7.50209500	-1.24298400	-1.34495100
C	6.68893900	-2.33064800	-1.01483800
C	5.35774000	-2.12812900	-0.64870000
C	3.19196900	-3.06889700	2.45915800
C	3.90879200	-3.68118800	3.48793100
C	5.02309300	-3.04570900	4.04313000
C	5.41333200	-1.79322800	3.56096800
C	4.70261900	-1.18567400	2.52524800
C	-4.03531900	-0.58155500	-0.51449600
C	-3.18601400	0.28452400	-1.17810700
C	-3.40877800	0.38767700	-2.56439500
C	-4.45444600	-0.37769500	-3.05964300
S	-5.20315100	-1.34117000	-1.70164900
C	-4.87966700	-0.39119300	-4.41440900
C	-5.91264000	-1.05660200	-5.03002700
C	-6.11997400	-0.89013400	-6.43424500
N	-6.28106500	-0.74713700	-7.58294600
C	-6.82101000	-1.91913300	-4.34860300
N	-7.57343000	-2.62558700	-3.79958600
H	-7.76757700	-1.52218200	4.48613300
H	-8.48645100	-1.07717000	2.13142800

H	-6.78371000	-0.79566400	0.34971100
H	-5.32459700	-1.65328300	5.02044000
H	-1.59823000	-1.94956300	-0.49456600
H	0.82549100	-1.93454500	-0.86384400
H	1.43328500	-0.44869500	3.11286000
H	-1.01459800	-0.43253600	3.47227100
H	3.28850100	-0.76370400	-2.96091300
H	2.08412600	0.70581800	-4.53889500
H	0.75997300	2.62971400	-3.68965400
H	0.64507200	3.05595600	-1.24277800
H	1.81984700	1.55975600	0.33276800
H	5.22598500	1.25192200	-0.95512500
H	7.59001600	0.89714400	-1.57576600
H	8.53480200	-1.40056400	-1.62640300
H	7.08926400	-3.33552800	-1.04431000
H	4.73482200	-2.97389100	-0.39379000
H	2.32274500	-3.56074800	2.04360100
H	3.59575900	-4.64866000	3.85805600
H	5.57550700	-3.51685800	4.84525200
H	6.26757900	-1.28826100	3.99250600
H	5.00965100	-0.21657100	2.15812000
H	-2.41751500	0.83630100	-0.66073700
H	-2.82447500	1.03165300	-3.20630300
H	-4.27734000	0.23441800	-5.06484900

Cell-imaging Details

Materials:

Dulbecco's modified eagle's media (DMEM), trypsin-EDTA solution (0.25% trypsin and 0.02% EDTA in DPBS), fetal bovine serum (FBS), dulbecco's phosphate-buffer saline (DPBS), and antibiotic antimycotic solution (10000 units of penicillin, 10.0 mg of streptomycin, and 25 µg of amphoterin B per mL in 0.9% normal saline), dimethyl sulfoxide (DMSO) (≥99.5%), trypan blue, and 3-(4,5-dimethylthiazol-2-yl)-2,5-diphenyl tetrazolium bromide (MTT) were purchased from HiMedia, India.

Cells and culture conditions:

Mouse fibroblast cell line (L929) and human triple-negative breast cancer cell line (MDA-MB-231) were procured from NCCS, Pune, India. The cells were cultured with complete DMEM (DMEM supplemented with 10% v/v FBS and 1% v/v antibiotic antimycotic solution), and the incubation conditions were 37°C and 5% CO_2.

Methods:

Biocompatibility and cytotoxicity assay

The colorimetric 3-(4,5-dimethylthiazol-2-yl)-2,5-diphenyl tetrazolium bromide (MTT) assay was carried out to check the cell viability/toxicity. L929 (mouse fibroblast cell lines) and MDA-MB 231 cells were used to analyze the cell viability and cytotoxicity assay, respectively. The cells were cultured in complete DMEM and were harvested by trypsinization for seeding in the well plate. Briefly, the cellular suspension of ~8,000-10,000 cells/well was seeded in a 96-well plate. Then, the cells were incubated for 24 hours to facilitate the cellular attachment on the surface of the well at 37 °C with 5% CO_2. After one wash with sterile phosphate buffer, different concentrations (10-100 µg/ml) of luminogens like GBY-12, GBY-14, GBY-13, GBY-15 were added into the wells in a triplicate manner. For positive control, 0.5 % triton X-100 and for growth/negative control, complete DMEM media were used. After 24 hours of treatment with the luminogens the samples were removed, and two gentle PBS washes were given to cells to remove the test samples properly. MTT solution (50 µg/well) was added to each well and further incubated for 2 hours (facilitates the conversion of MTT to formazan). Afterward, DMSO was added to each well to dissolve formazan. The formazan's optical density (OD) was then measured at 570 nm using a plate reader (Tecan Infinite M200 Pro). Depending upon the OD data, cellular viability was calculated for the luminogen-treated wells. [3-4]

Percentage cell viability was calculated using the following equation:

$$Cell\ Viability\ (\%) = \frac{Fluorescence\ intensity\ of\ test\ sample}{Fluorescence\ intensity\ of\ negative\ control} \times 100$$

where test sample intensities are the intensity of the compound.

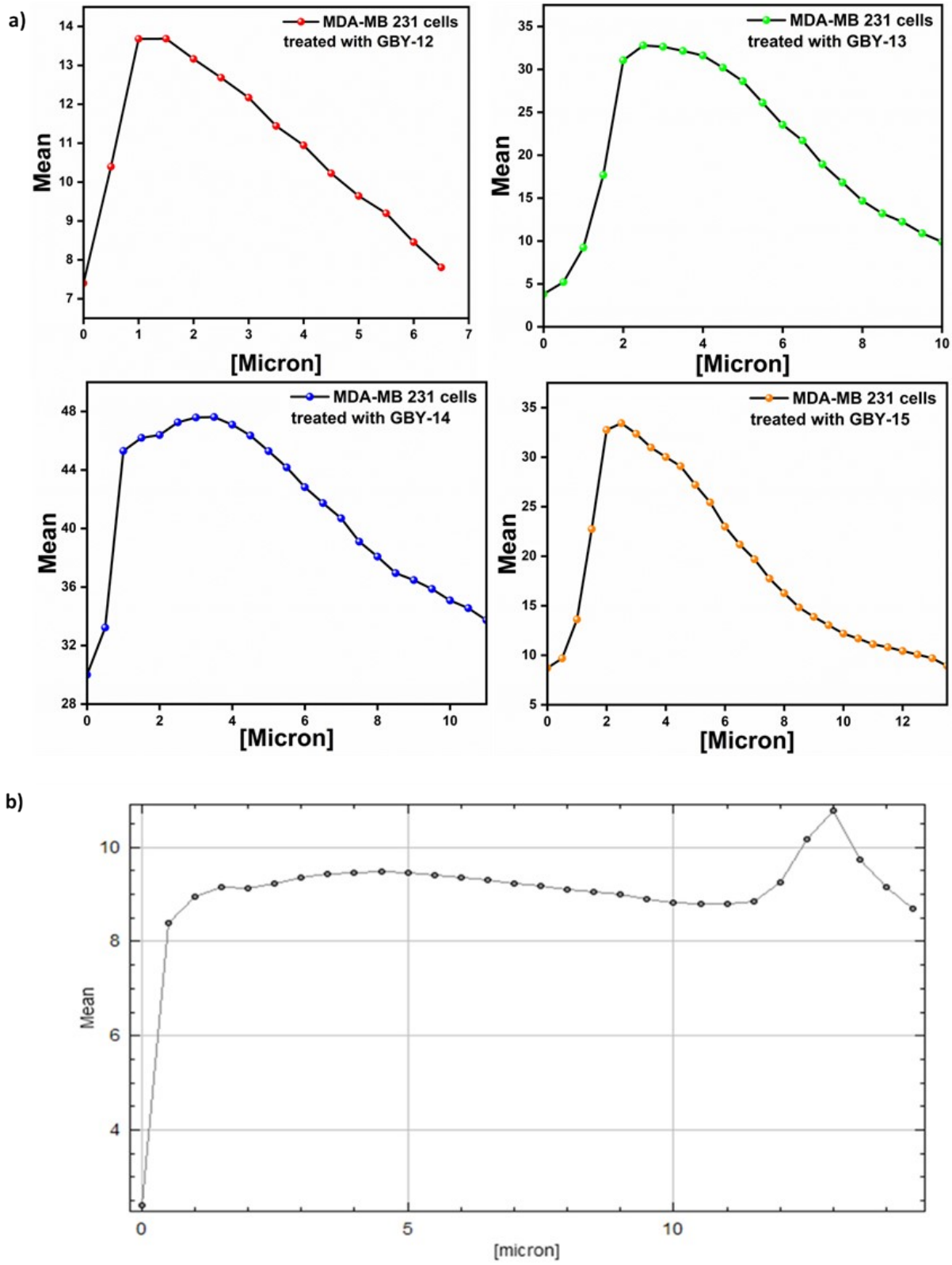

Figure S17. a) Fluorescence intensity comparison between **GBY-12**, **GBY-13**, **GBY-14,** and **GBY-15; b)** Mean Green Fluorescence Intensity of control cells.

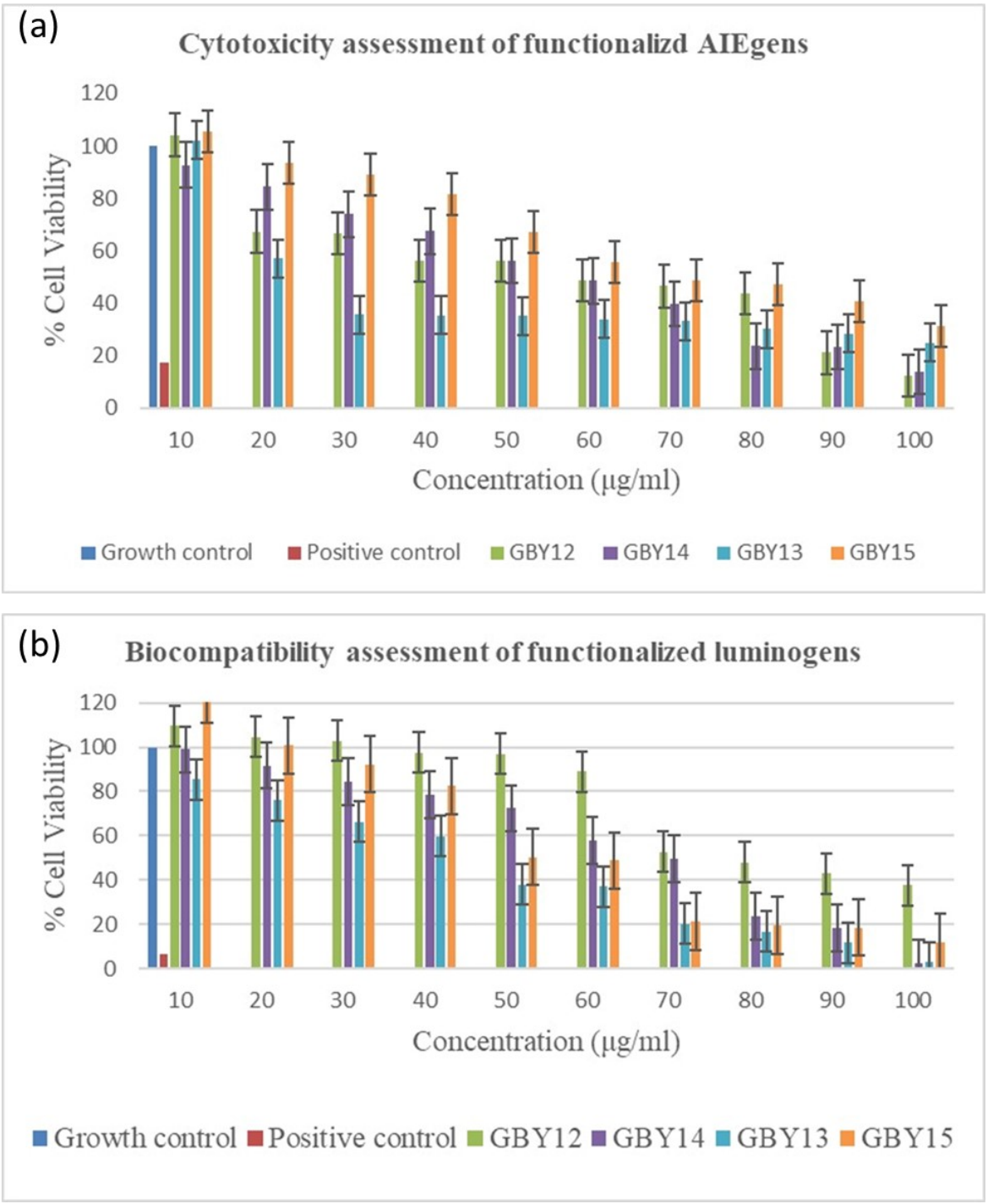

Figure. S18. (a) Comparative *in-vitro* cell viability studies on L929 cells reveal the concentration-dependent cytotoxic response of AIEgens **GBY-12, GBY-13, GBY-14,** and **GBY-15; (b)** *In-vitro* anticancer activity of AIEgens on MDA-MB 231 cells (Note: The results have also been presented as mean±SD. The SD is denoted by the error bar).

Hydrazine sensing

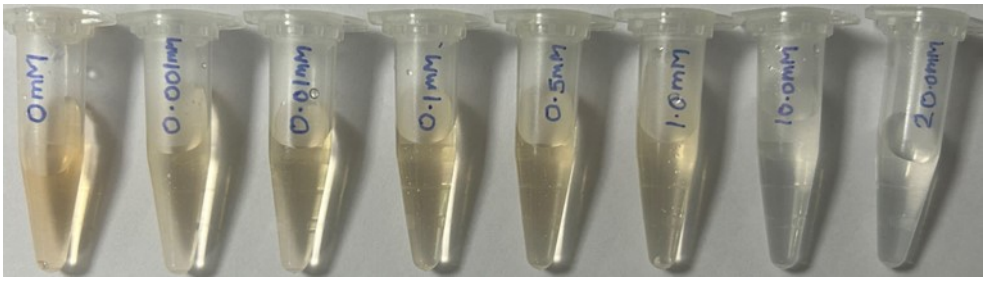

Figure S19. A distinct color change of luminogen **GBY-15** observable to the naked eye across different concentrations of hydrazine

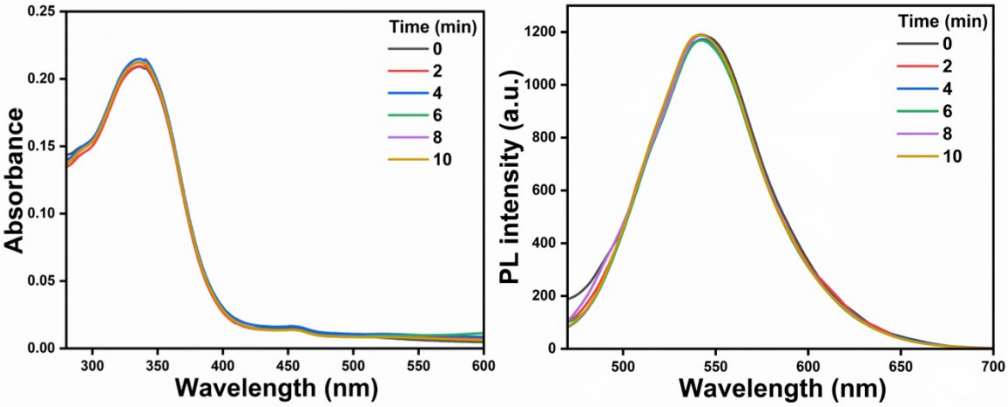

Figure S20. Photostability of **GBY-15** in a 10 mM hydrazine hydrate solution.

Limit of detection

Detection limit calculations for **GBY-15** (1 mM) in THF with N_2H_4 (0 to 0.4 mM) in THF:Water (9.5:0.5 v/v)

σ = Standard Deviation obtained from 10 blank emission measurement of THF:Water (9.5:0.5 v/v)

σ = 6.026

and k is slope obtained from Plot of emission intensity of **GBY-15** in THF:Water (9.5:0.5 v/v) at 465 nm versus concentration of N_2H_4 in THF

k = 1344.822

Detection limit = 3σ/k

Detection limit = 3*6.026/1344.822

Detection limit = 0.013 mM

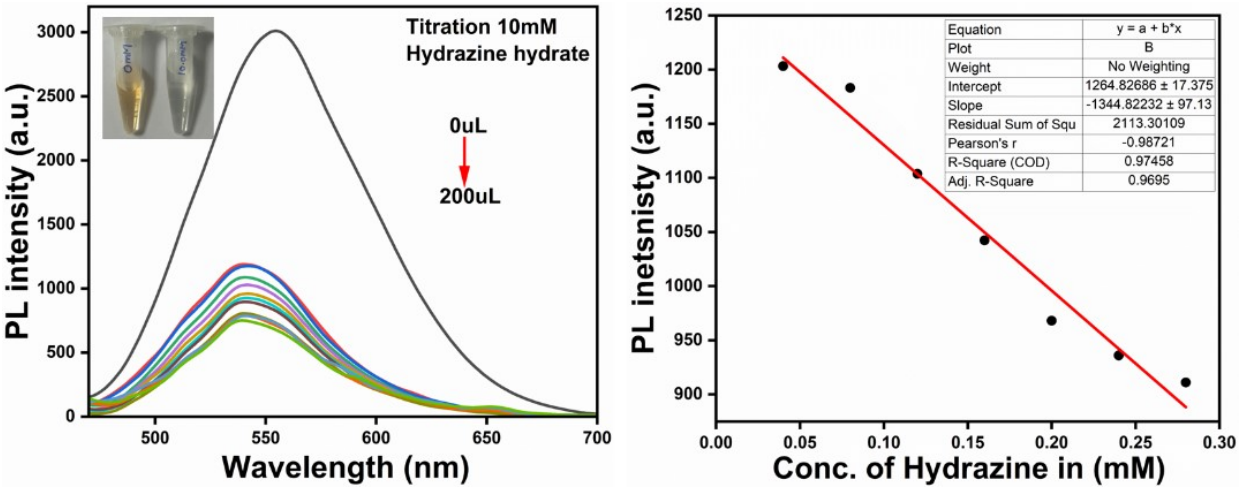

Figure S21. Titration of hydrazine with **GBY-15** in aggregated state and Plot of hydrazine concentration vs PL intensity

References:

1. (a) Z. Lu, Y. Liu, S. Lu, Y. Li, X. Liu, Y. Qin and L. Zheng, A highly selective TPE-based AIE fluorescent probe is developed for the detection of Ag+, *RSC Adv.*, 2018, **8**, 19701– 19706. (b) G. Yashwantrao, P. Shetty, P. J. Maleikal, P. Badani, S. Saha, Dehydrative Substitution Reaction in Water for the Preparation of Unsymmetrically Substituted Triarylmethanes: Synthesis, Aggregation-Enhanced Emission, and Mechanofluorochromism, *ChemPlusChem*, 2022, **87**, 7, e202200150. (c) V.P. Jejurkar, G. Yashwantrao, P.K. Reddy, A.P. Ware, S.S. Pingale, R. Srivastava and S. Saha, Rationally Designed Furocarbazoles as Multifunctional Aggregation Induced Emissive Luminogens for the Sensing of Trinitrophenol (TNP) and Cell-imaging, *ChemPhotoChem.*, 2020, **4**, 691-703
2. M. J. Frisch, G. W. Trucks, H. B. Schlegel, G. E. Scuseria, M. A. Robb, J. R. Cheeseman, G. Scalmani, V. Barone, B. Mennucci, G. A. Petersson, H. Nakatsuji, M. Caricato, X. Li, H. P. Hratchian, A. F. Izmaylov, J. Bloino, G. Zheng, J. L. Sonnenberg, M. Hada, M. Ehara, K. Toyota, R. Fukuda, J. Hasegawa, M. Ishida, T. Nakajima, Y. Honda, O. Kitao, H. Nakai, T. Vreven, J.A. Montgomery Jr., J. E. Peralta, F. Ogliaro, M. Bearpark, J. J. Heyd, E. Brothers, K.N. Kudin, V. N. Staroverov, R. Kobayashi, J. Normand, K. Raghavachari, A. Rendell, J.C. Burant, S.S. Iyengar, J. Tomasi, M. Cossi, N. Rega, J. M. Millam, M. Klene, J.E. Knox, J.B. Cross, V. Bakken, C. Adamo, J. Jaramillo, R. Gomperts, R. E. Stratmann, O. Yazyev, A. J. Austin, R. Cammi, C. Pomelli, J. W. Ochterski, R. L. Martin, K. Morokuma, V. G. Zakrzewski, G. A. Voth, P. Salvador, J. J. Dannenberg, S. Dapprich, A. D. Daniels, O. Farkas, J. B. Foresman, J. V. Ortiz, J. Cioslowski and D. J. Fox, *Gaussian 16, Revision A*. 03, Gaussian, Inc., Wallingford CT, **2016**.
3. D. S. Chauhan, B. P. K. Reddy, S. K. Mishra, R. Prasad, M. Dhanka, M. Vats, G. Ravichandran, D. Poojari, O. Mhatre, A. De and Rohit Srivastava, A Comprehensive Evaluation of Degradable and Cost Effective Plasmonic Nanoshells for Localized Photothermolysis of Cancer Cells, *Langmuir.*, 2019, **35**, 24, 7805–7815. DOI: 10.1021/acs.langmuir.8b03460
4. M. K. Kumawat, M. Thakur, R. B. Gurung and R. Srivastava Graphene quantum dots from Mangifera indica: application in near-infrared bioimaging and intracellular nano thermometry *ACS Sustain. Chem. Eng.*, 2017, **5**, 1382-1391.

^{1}H and ^{13}C NMR Spectral Reproductions Of 3, 5, GBY-12, GBY-13, GBY-14 and GBY-15

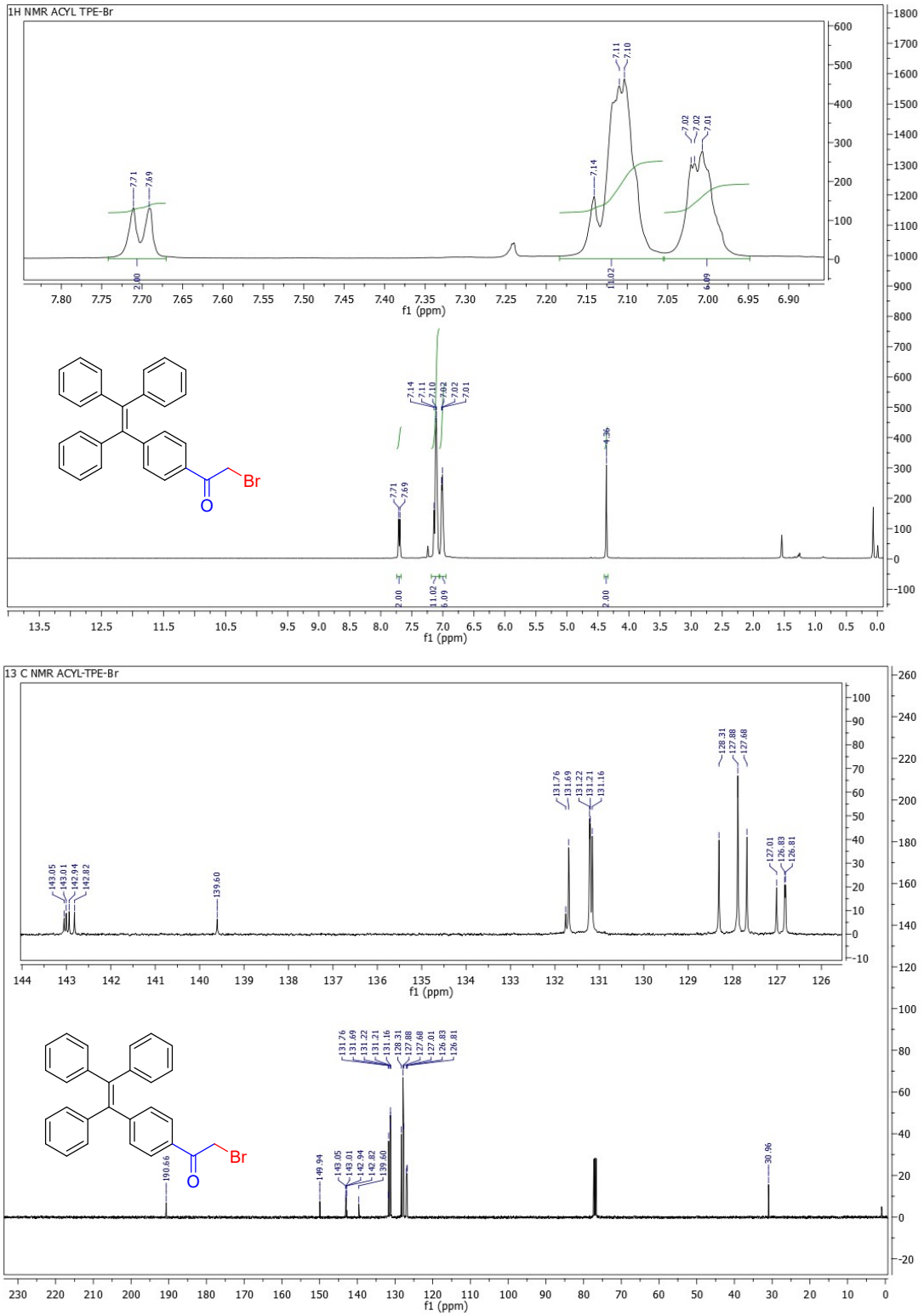

Figure S22. ^{1}H (400 MHz,$CDCl_3$) and ^{13}C NMR (100 MHz,$CDCl_3$) spectral reproduction of 2-bromo-1-(4-(1,2,2-triphenylvinyl)phenyl)ethan-1-one (**3**).

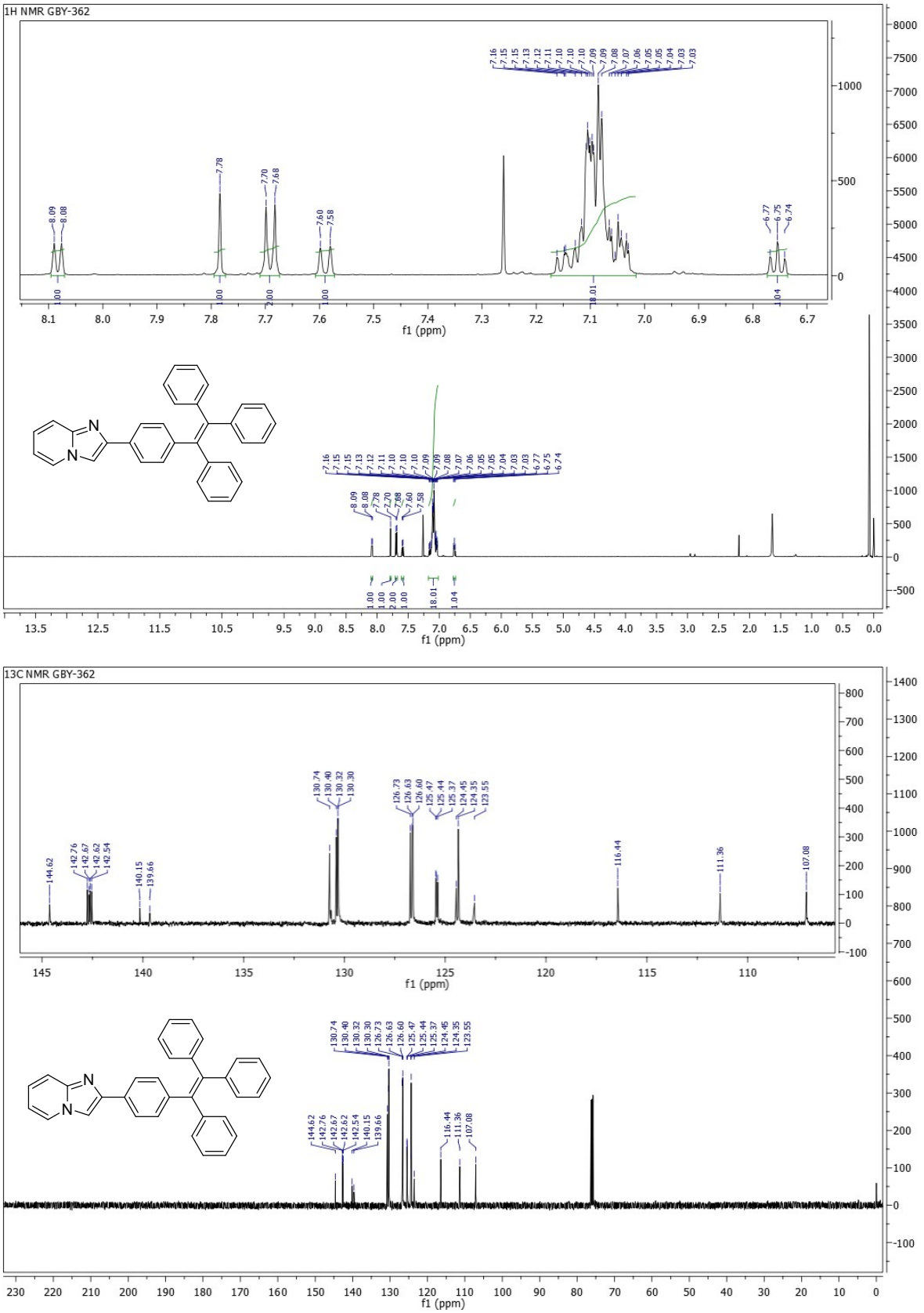

Figure S23. ^{1}H NMR (500 MHz, $CDCl_3$) and ^{13}C NMR (126 MHz, $CDCl_3$) spectral reproduction of 2-(4-(1,2,2-triphenylvinyl)phenyl)imidazo[1,2-a]pyridine **(5).**

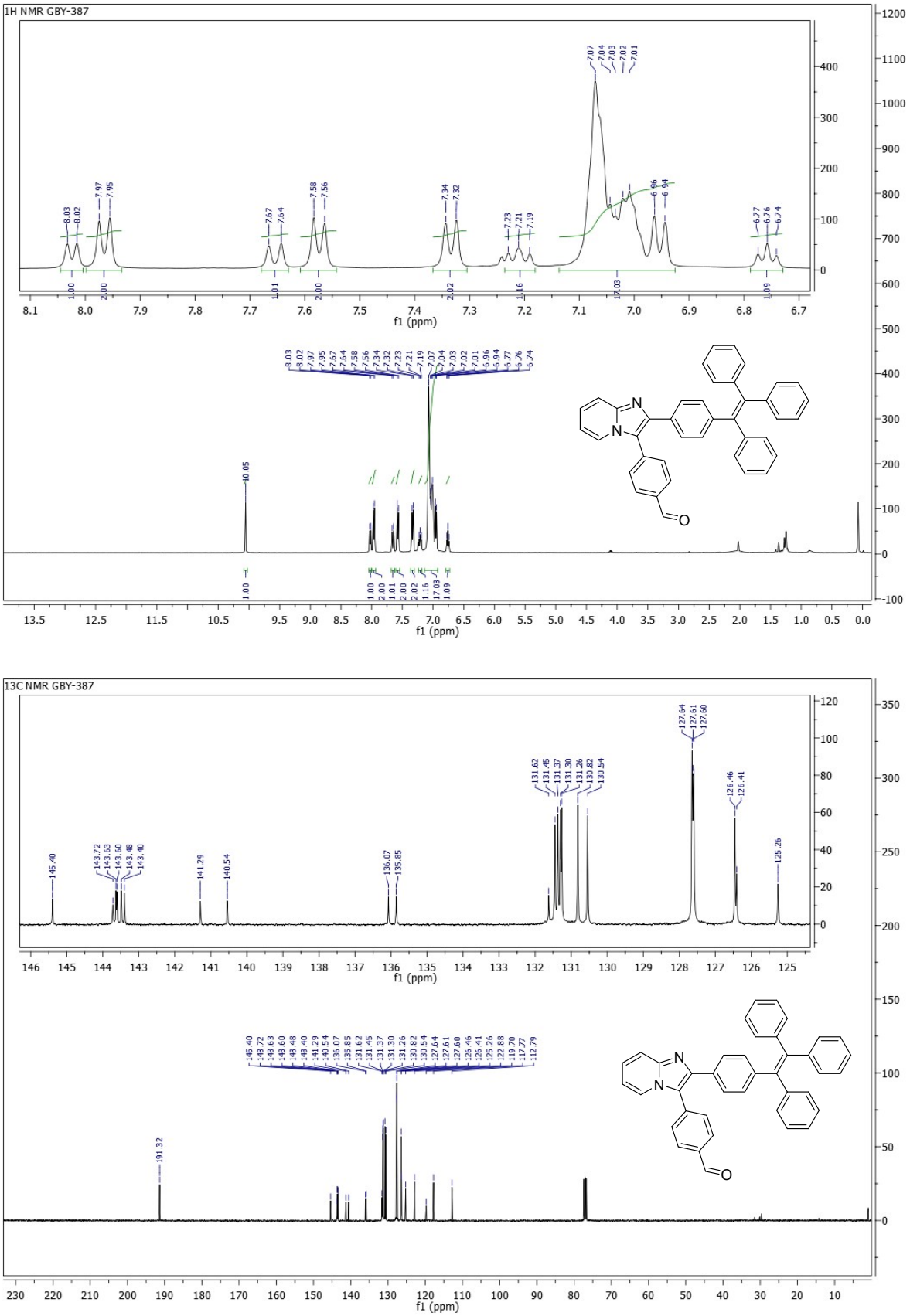

Figure S24. ^{1}H NMR (500 MHz, $CDCl_3$) and ^{13}C NMR (126 MHz, $CDCl_3$) spectral reproduction of 4-(2-(4-(1,2,2-triphenylvinyl)phenyl)imidazo[1,2-a]pyridin-3-yl)benzaldehyde **(GBY-12).**

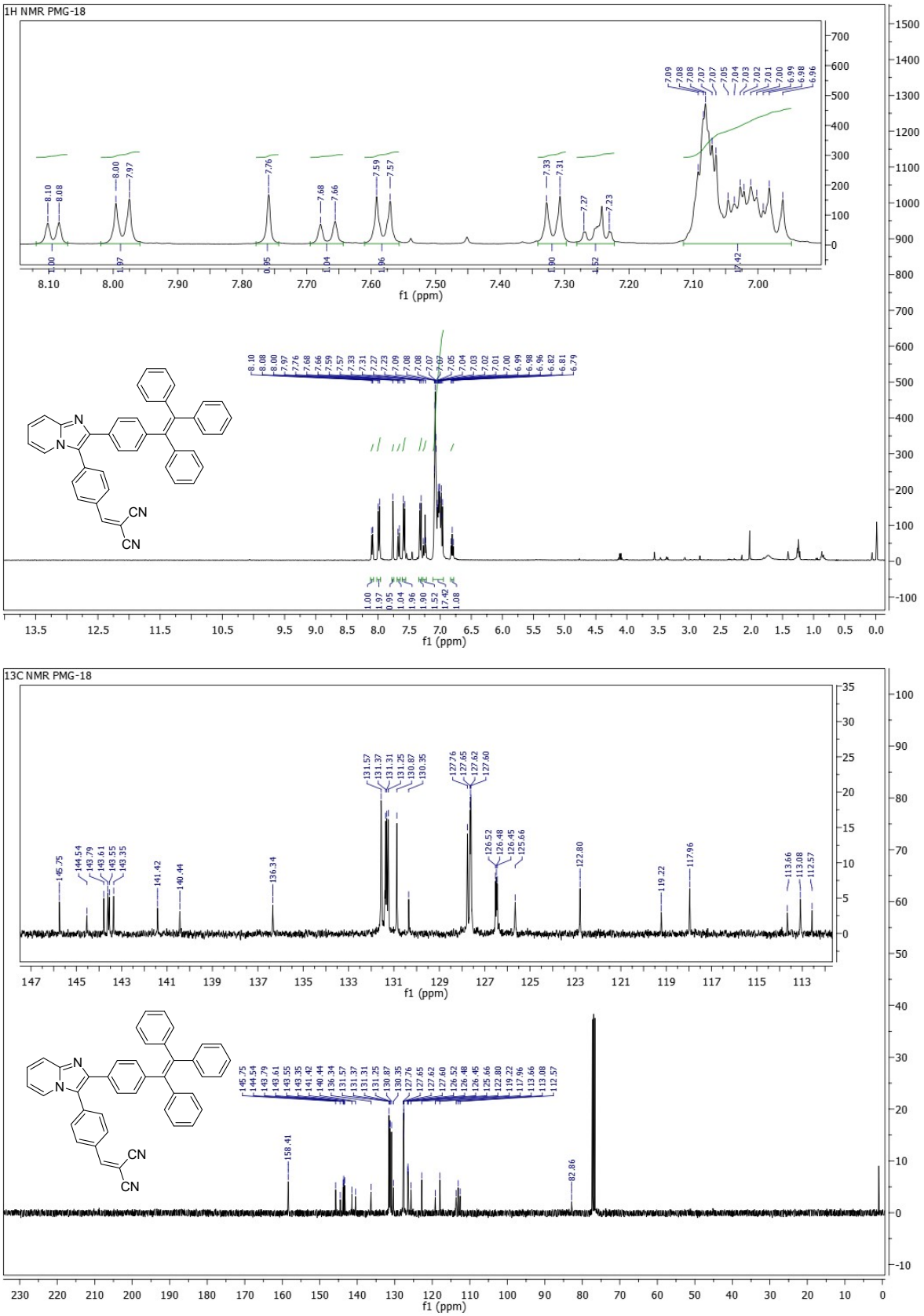

Figure S25. ^{1}H NMR (400 MHz, $CDCl_3$) and ^{13}C NMR (101 MHz, $CDCl_3$) spectral reproduction of 2-(4-(2-(4-(1,2,2-triphenylvinyl)phenyl)imidazo[1,2-a]pyridin-3-yl)benzylidene)malononitrile **(GBY-13)**.

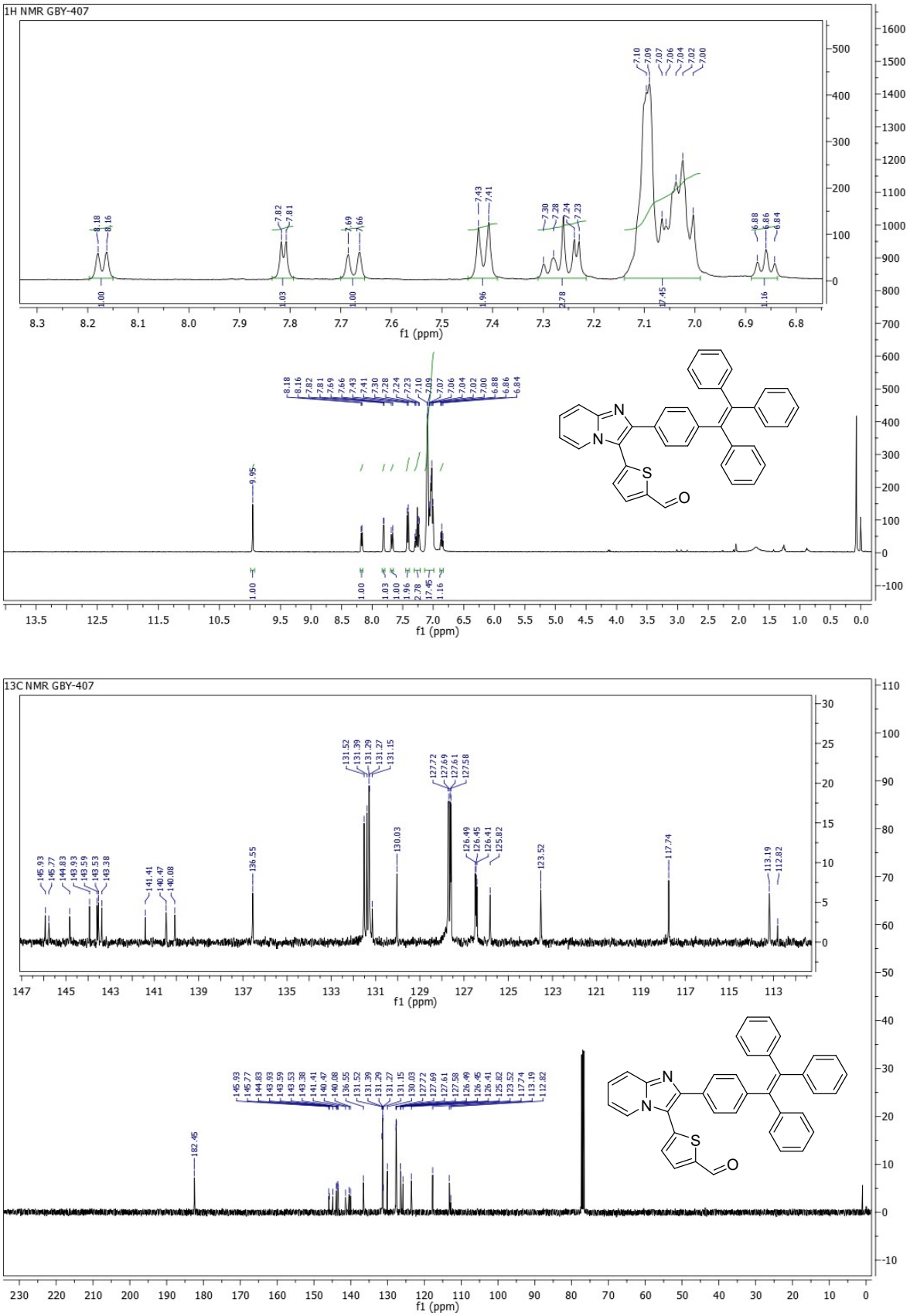

Figure S26. ^{1}H NMR (400 MHz, $CDCl_3$) and ^{13}C NMR (101 MHz, $CDCl_3$) spectral reproduction of 5-(2-(4-(1,2,2-triphenylvinyl)phenyl)imidazo[1,2-a]pyridin-3-yl)thiophene-2-carbaldehyde **(GBY-14).**

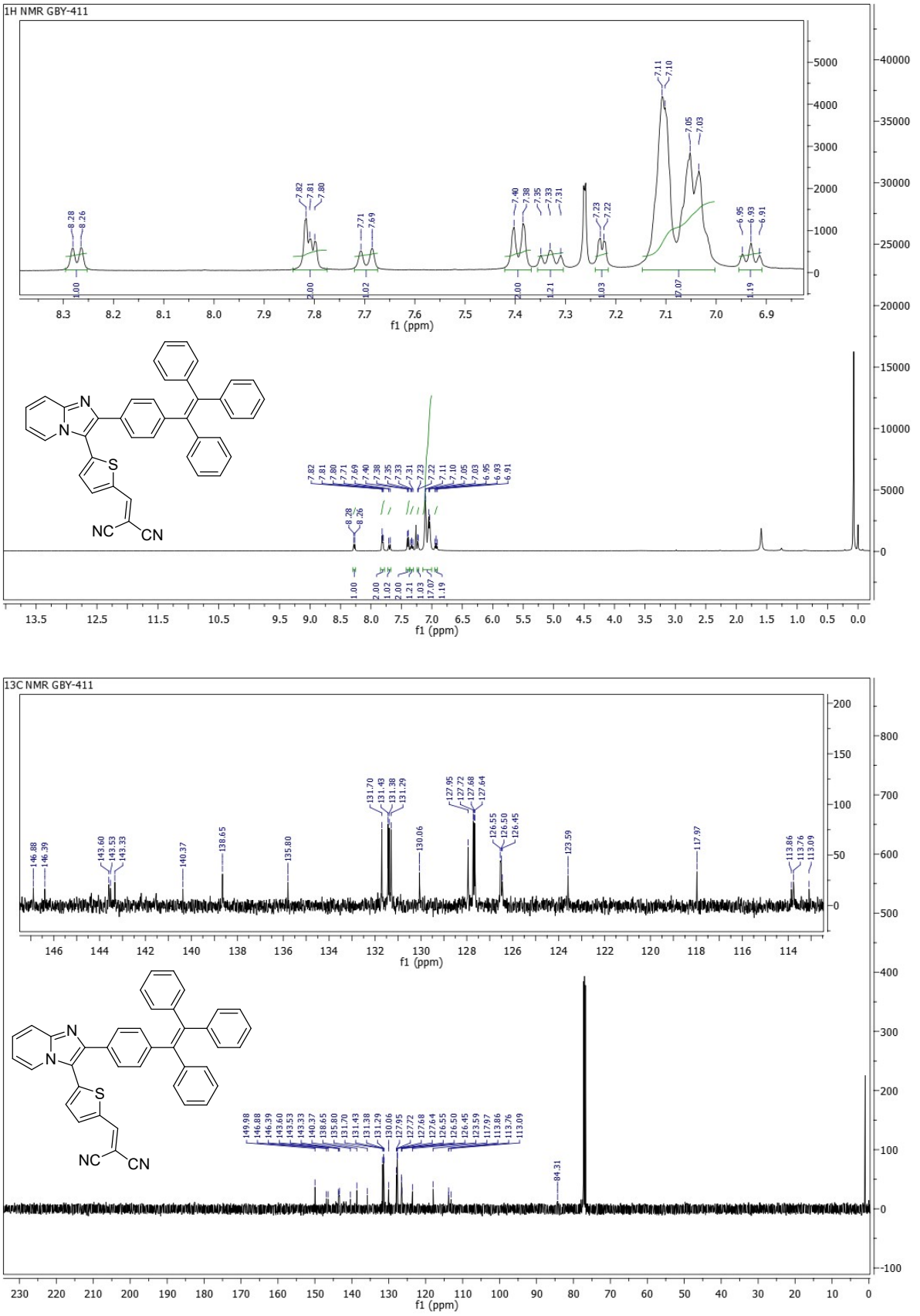

Figure S27. ^{1}H NMR (400 MHz, $CDCl_3$) and ^{13}C NMR (126 MHz, $CDCl_3$) spectral reproduction of 2-((5-(2-(4-(1,2,2-triphenylvinyl)phenyl)imidazo[1,2-a]pyridin-3-yl)thiophen-2-yl)methylene)malononitrile **(GBY-15).**

LC-HRMS data of 3, 5, GBY-12, GBY-13, GBY-14, GBY-15

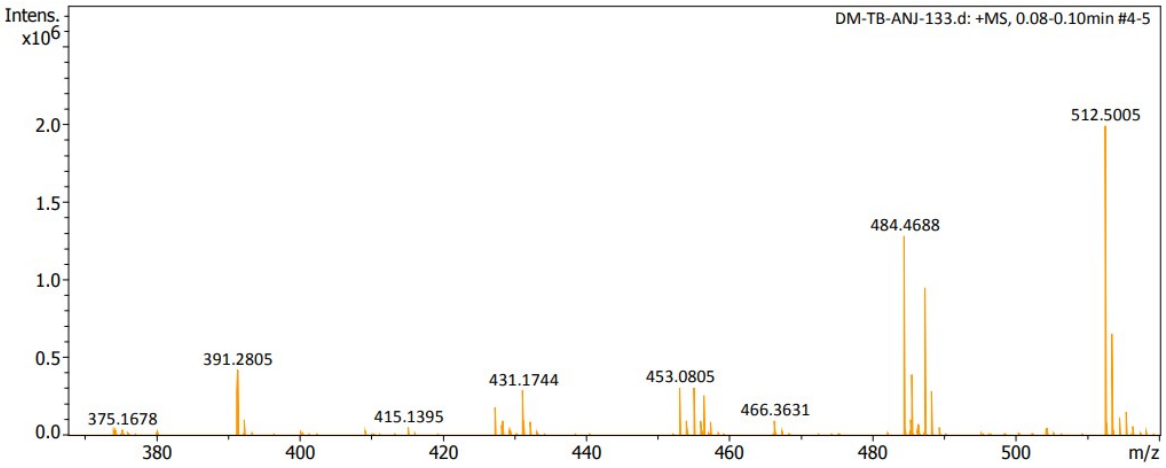

Figure S28. HR-LC-MS spectra of **3**.

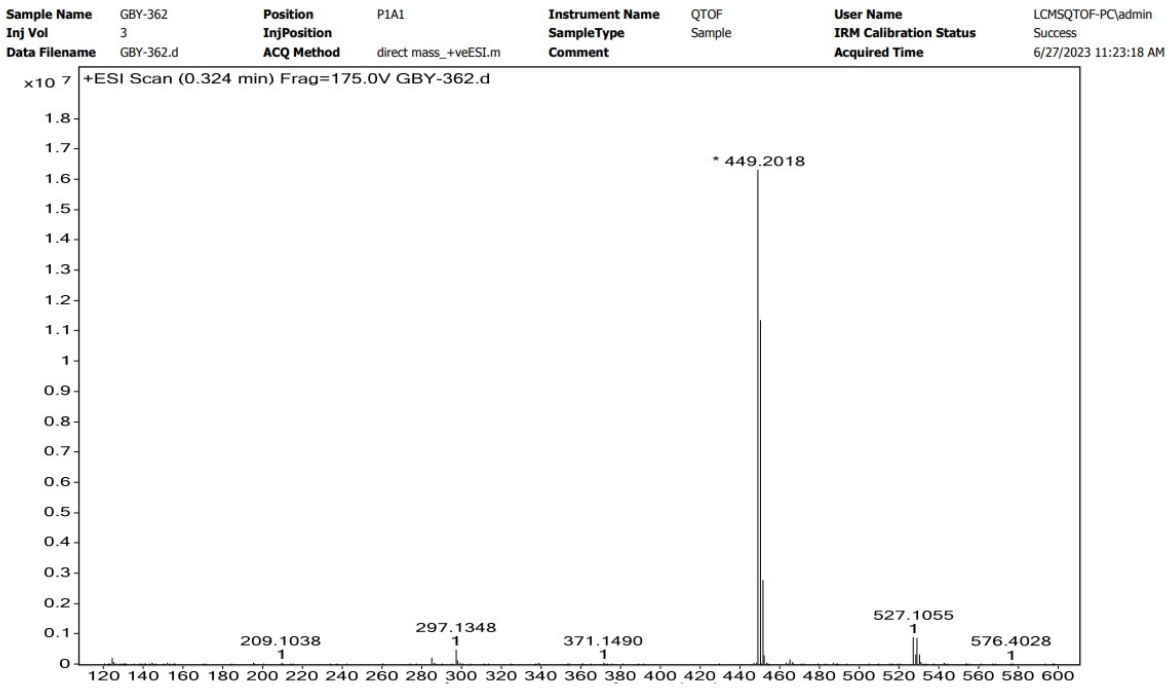

Figure S29. HR-LC-MS spectra of **5**.

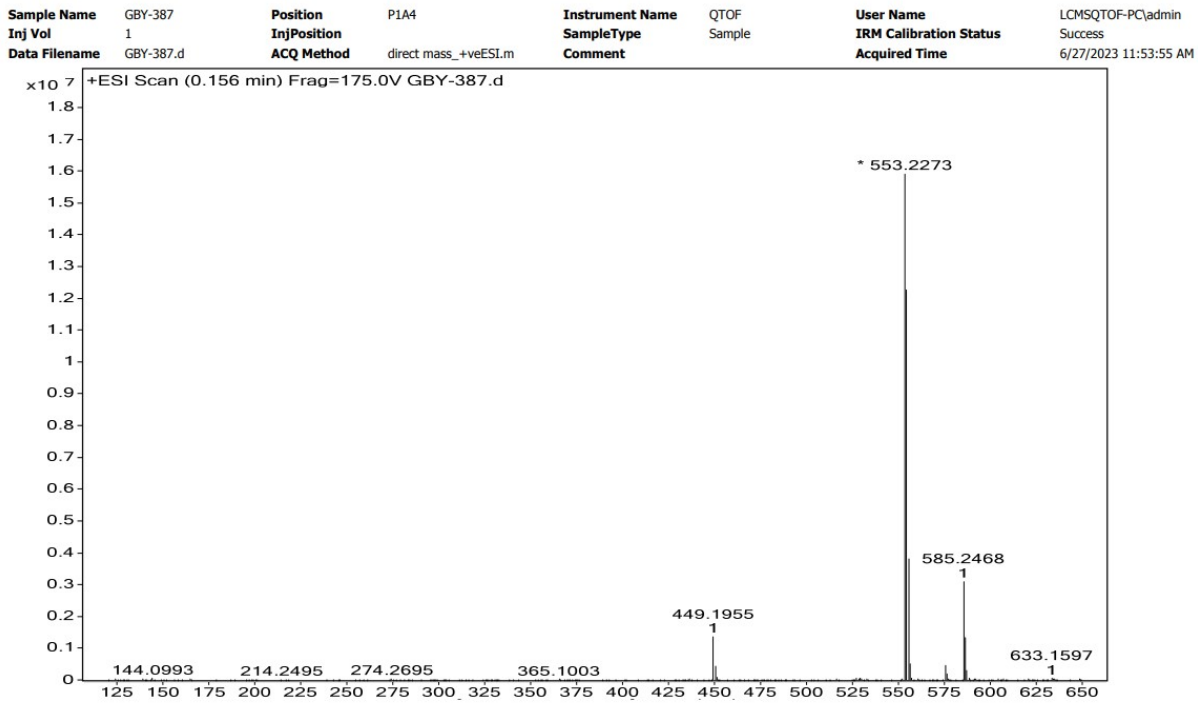

Figure S30. HR-LC-MS spectra of **GBY-12**.

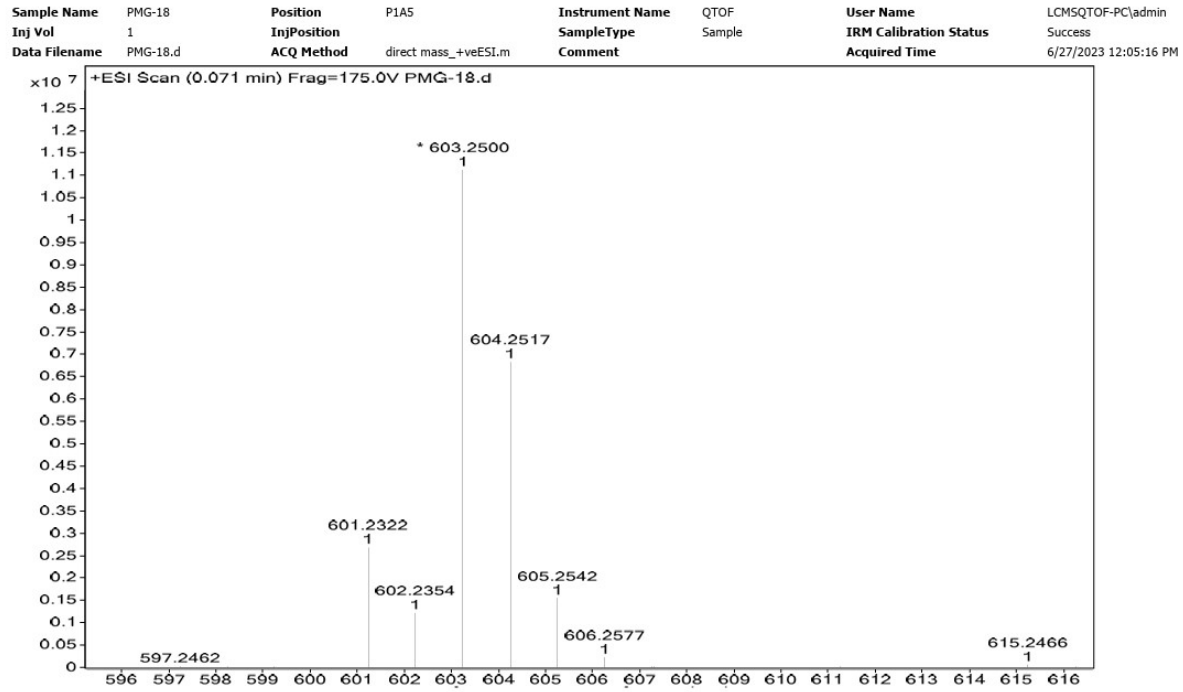

Figure S31. HR-LC-MS spectra of **GBY-13**.

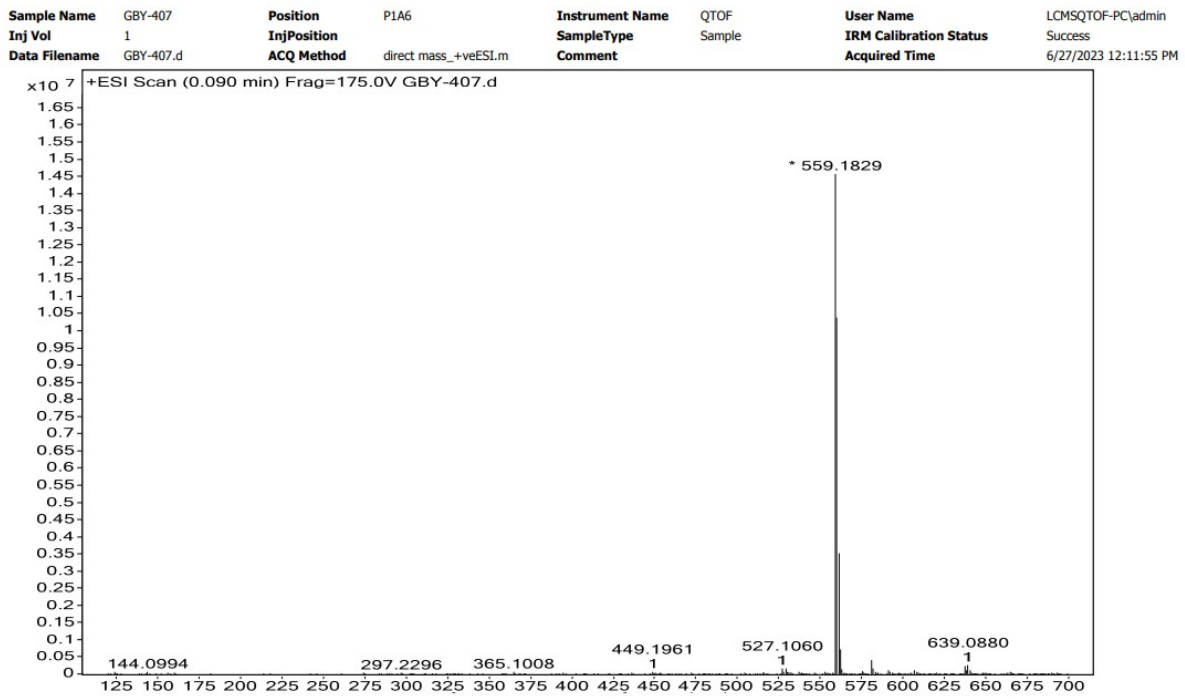

Figure S32. HR-LC-MS spectra of **GBY-14**.

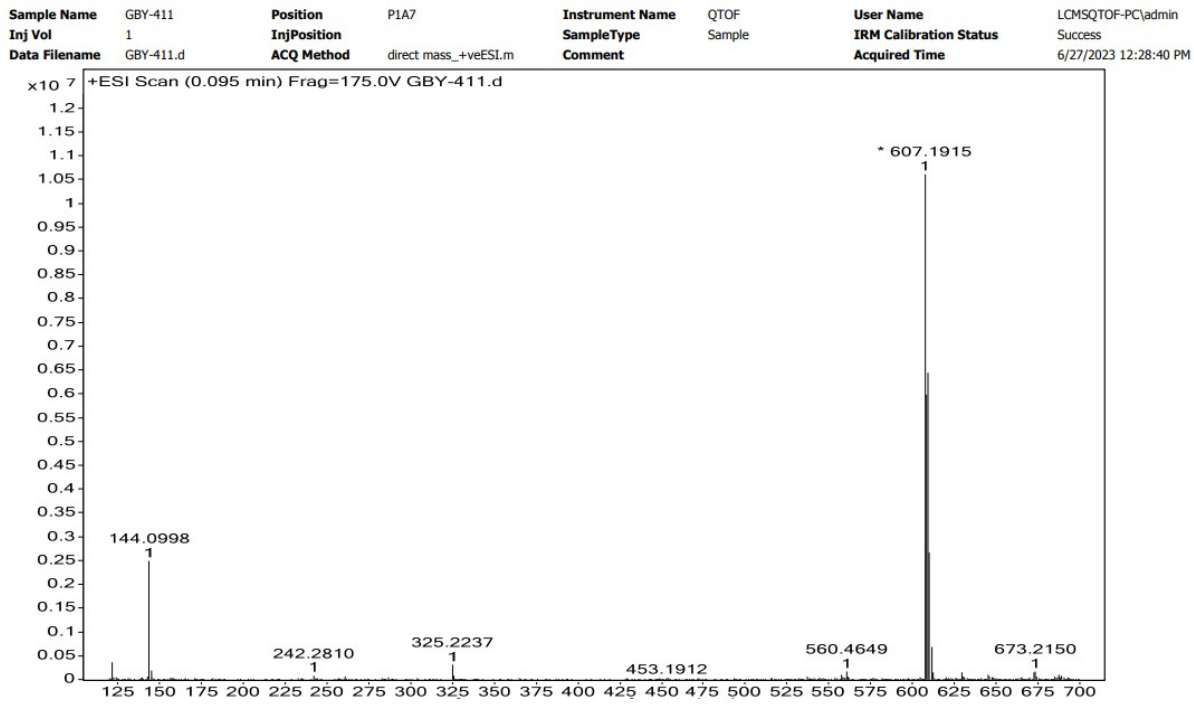

Figure S33. HR-LC-MS spectra of **GBY-15**.

Single Crystal XRD Analysis of GBY-12 and GBY-14

The Single crystal XRD data has been collected on single crystal X-ray diffractometer of Bruker Smart Apex Duo diffractometer at 100 K using Mo Kα radiation (λ = 0.71073 Å). The frames were integrated with the Bruker SAINT Software package using a narrow-frame algorithm. Data were corrected for absorption effects using the Multi-Scan method (SADABS). The structure was solved and refined using the Bruker SHELXTL Software Package. The structure figure was generated with ORTEP.

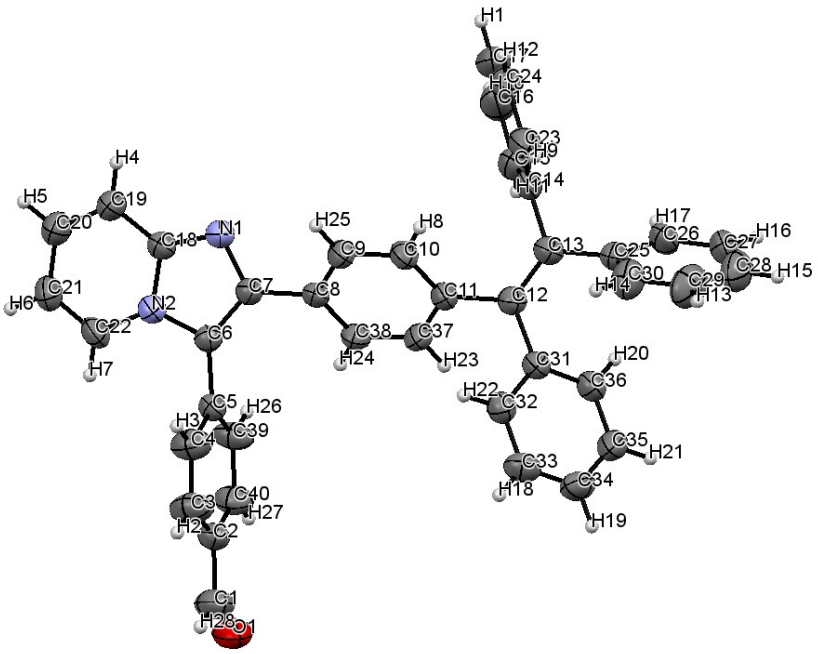

Figure S34. X-Ray crystal structure of **GBY-12** (Ellipsoids with 50% probability).

Table S7. Single crystal data and structure refinement for **GBY-12**.

Identification code	2382091
Empirical formula	$C_{40}H_{28}ON_2$
Formula weight	552.64
Temperature	296K
Wavelength	0.7107
Crystal system	Triclinic
Space group	P -1
Unit cell dimensions	
a(Å)	9.475 (11)

b(Å)	10.788 (15)
c(Å)	15.1924 (19)
α(Å)	74.047 (4)
β(Å)	79.474 (3)
γ(Å)	79.956 (3)
Volume	1455.4 (3)
Z	2
Density (calculated)	1.261
Absorption coefficient	0.075
F(000)	580
Refinement method	SHELXL 2017/1 (Sheldrick, 2017)
Data / restraints / parameters	8009/0/388
Goodness-of-fit on F2	0.948
Final R indices [I>2sigma(I)]	R1 = 0.0873, wR2 = 0.1416
R indices (all data)	R1 = 0.1766, wR2 = 0.1677

$$R_1 = \frac{\sum \| F_0| - |F_c \|}{\sum |F_0|}$$

$$R_w = \sqrt{\frac{\left[\sum \{w(F_0^2 - F_c^2)^2\}\right]}{\left[\sum \{w(F_0^2)^2\}\right]}}$$

Table S8. List Torsion angles [°] for luminogen **GBY-12**

Number	Atom1	Atom2	Atom3	Atom4	Torsion
1	C18	N1	C7	C6	-0.1(4)
2	C18	N1	C7	C8	178.7(3)
3	C7	N1	C18	N2	0.2(4)

4	C7	N1	C18	C19	-175.7(4)
5	C18	N2	C6	C5	178.9(3)
6	C18	N2	C6	C7	0.1(4)
7	C22	N2	C6	C5	-4.0(6)
8	C22	N2	C6	C7	177.2(4)
9	C6	N2	C18	N1	-0.1(4)
10	C6	N2	C18	C19	176.4(3)
11	C22	N2	C18	N1	-177.6(3)
12	C22	N2	C18	C19	-1.1(5)
13	C6	N2	C22	C21	-175.4(4)
14	C6	N2	C22	H7	4.5
15	C18	N2	C22	C21	1.3(6)
16	C18	N2	C22	H7	-178.7
17	O1	C1	C2	C3	179.3(5)
18	O1	C1	C2	C40	0.2(7)
19	H28	C1	C2	C3	-0.6
20	H28	C1	C2	C40	-179.7
21	C1	C2	C3	H2	-0.3
22	C1	C2	C3	C4	179.6(4)
23	C40	C2	C3	H2	178.7
24	C40	C2	C3	C4	-1.3(6)
25	C1	C2	C40	C39	179.8(4)
26	C1	C2	C40	H27	-0.1
27	C3	C2	C40	C39	0.7(6)
28	C3	C2	C40	H27	-179.2
29	C2	C3	C4	H3	-179.4
30	C2	C3	C4	C5	0.8(7)

31	H2	C3	C4	H3	0.6
32	H2	C3	C4	C5	-179.3
33	C3	C4	C5	C6	176.3(4)
34	C3	C4	C5	C39	0.5(6)
35	H3	C4	C5	C6	-3.6
36	H3	C4	C5	C39	-179.4
37	C4	C5	C6	N2	-78.8(4)
38	C4	C5	C6	C7	99.7(5)
39	C39	C5	C6	N2	96.9(4)
40	C39	C5	C6	C7	-84.7(5)
41	C4	C5	C39	H26	178.9
42	C4	C5	C39	C40	-1.1(6)
43	C6	C5	C39	H26	3.1
44	C6	C5	C39	C40	-177.0(4)
45	N2	C6	C7	N1	0.0(4)
46	N2	C6	C7	C8	-178.6(3)
47	C5	C6	C7	N1	-178.6(3)
48	C5	C6	C7	C8	2.8(6)
49	N1	C7	C8	C9	36.2(4)
50	N1	C7	C8	C38	-141.9(3)
51	C6	C7	C8	C9	-145.3(4)
52	C6	C7	C8	C38	36.7(5)
53	C7	C8	C9	H25	1.6
54	C7	C8	C9	C10	-178.5(3)
55	C38	C8	C9	H25	179.7
56	C38	C8	C9	C10	-0.3(5)
57	C7	C8	C38	C37	178.2(3)

58	C7	C8	C38	H24	-1.7
59	C9	C8	C38	C37	0.1(5)
60	C9	C8	C38	H24	-179.8
61	C8	C9	C10	H8	-179
62	C8	C9	C10	C11	1.0(6)
63	H25	C9	C10	H8	1
64	H25	C9	C10	C11	-179.1
65	C9	C10	C11	C12	-177.3(3)
66	C9	C10	C11	C37	-1.3(5)
67	H8	C10	C11	C12	2.7
68	H8	C10	C11	C37	178.7
69	C10	C11	C12	C13	-45.0(6)
70	C10	C11	C12	C31	132.9(4)
71	C37	C11	C12	C13	139.2(4)
72	C37	C11	C12	C31	-42.9(5)
73	C10	C11	C37	H23	-178.9
74	C10	C11	C37	C38	1.1(6)
75	C12	C11	C37	H23	-2.8
76	C12	C11	C37	C38	177.2(3)
77	C11	C12	C13	C14	-6.3(6)
78	C11	C12	C13	C25	173.6(3)
79	C31	C12	C13	C14	176.0(3)
80	C31	C12	C13	C25	-4.1(6)
81	C11	C12	C31	C32	-43.9(5)
82	C11	C12	C31	C36	134.3(4)
83	C13	C12	C31	C32	134.0(4)
84	C13	C12	C31	C36	-47.8(5)

85	C12	C13	C14	C15	-66.9(6)
86	C12	C13	C14	C23	115.0(4)
87	C25	C13	C14	C15	113.2(4)
88	C25	C13	C14	C23	-65.0(5)
89	C12	C13	C25	C26	115.9(4)
90	C12	C13	C25	C30	-63.4(5)
91	C14	C13	C25	C26	-64.2(5)
92	C14	C13	C25	C30	116.6(4)
93	C13	C14	C15	H11	2.2
94	C13	C14	C15	C16	-177.7(4)
95	C23	C14	C15	H11	-179.7
96	C23	C14	C15	C16	0.4(6)
97	C13	C14	C23	H9	-0.4
98	C13	C14	C23	C24	179.6(4)
99	C15	C14	C23	H9	-178.6
100	C15	C14	C23	C24	1.4(6)
101	C14	C15	C16	H10	178
102	C14	C15	C16	C17	-2.0(8)
103	H11	C15	C16	H10	-1.9
104	H11	C15	C16	C17	178.1
105	C15	C16	C17	H1	-178.3
106	C15	C16	C17	C24	1.7(8)
107	H10	C16	C17	H1	1.7
108	H10	C16	C17	C24	-178.3
109	C16	C17	C24	C23	0.1(8)
110	C16	C17	C24	H12	-180
111	H1	C17	C24	C23	-179.9

112	H1	C17	C24	H12	0
113	N1	C18	C19	H4	-3.9
114	N1	C18	C19	C20	176.1(4)
115	N2	C18	C19	H4	-179.5
116	N2	C18	C19	C20	0.5(5)
117	C18	C19	C20	H5	179.8
118	C18	C19	C20	C21	-0.1(6)
119	H4	C19	C20	H5	-0.2
120	H4	C19	C20	C21	179.9
121	C19	C20	C21	H6	-179.7
122	C19	C20	C21	C22	0.3(6)
123	H5	C20	C21	H6	0.4
124	H5	C20	C21	C22	-179.6
125	C20	C21	C22	N2	-0.9(6)
126	C20	C21	C22	H7	179.1
127	H6	C21	C22	N2	179.1
128	H6	C21	C22	H7	-0.9
129	C14	C23	C24	C17	-1.7(7)
130	C14	C23	C24	H12	178.4
131	H9	C23	C24	C17	178.4
132	H9	C23	C24	H12	-1.6
133	C13	C25	C26	H17	3.6
134	C13	C25	C26	C27	-176.4(4)
135	C30	C25	C26	H17	-177.1
136	C30	C25	C26	C27	2.9(6)
137	C13	C25	C30	C29	178.0(4)
138	C13	C25	C30	H14	-2

139	C26	C25	C30	C29	-1.3(6)
140	C26	C25	C30	H14	178.7
141	C25	C26	C27	H16	177.9
142	C25	C26	C27	C28	-2.1(7)
143	H17	C26	C27	H16	-2
144	H17	C26	C27	C28	177.9
145	C26	C27	C28	H15	179.7
146	C26	C27	C28	C29	-0.3(8)
147	H16	C27	C28	H15	-0.3
148	H16	C27	C28	C29	179.6
149	C27	C28	C29	H13	-178.1
150	C27	C28	C29	C30	1.9(8)
151	H15	C28	C29	H13	1.9
152	H15	C28	C29	C30	-178.1
153	C28	C29	C30	C25	-1.1(7)
154	C28	C29	C30	H14	178.9
155	H13	C29	C30	C25	178.9
156	H13	C29	C30	H14	-1.1
157	C12	C31	C32	H22	0.6
158	C12	C31	C32	C33	-179.5(4)
159	C36	C31	C32	H22	-177.8
160	C36	C31	C32	C33	2.1(6)
161	C12	C31	C36	C35	179.4(4)
162	C12	C31	C36	H20	-0.6
163	C32	C31	C36	C35	-2.3(6)
164	C32	C31	C36	H20	177.7
165	C31	C32	C33	H18	179

166	C31	C32	C33	C34	-1.0(6)
167	H22	C32	C33	H18	-1.1
168	H22	C32	C33	C34	178.9
169	C32	C33	C34	H19	179.8
170	C32	C33	C34	C35	-0.2(7)
171	H18	C33	C34	H19	-0.1
172	H18	C33	C34	C35	179.9
173	C33	C34	C35	H21	180
174	C33	C34	C35	C36	0.0(7)
175	H19	C34	C35	H21	0
176	H19	C34	C35	C36	-179.9
177	C34	C35	C36	C31	1.2(6)
178	C34	C35	C36	H20	-178.7
179	H21	C35	C36	C31	-178.7
180	H21	C35	C36	H20	1.3
181	C11	C37	C38	C8	-0.5(6)
182	C11	C37	C38	H24	179.4
183	H23	C37	C38	C8	179.5
184	H23	C37	C38	H24	-0.6
185	C5	C39	C40	C2	0.6(6)
186	C5	C39	C40	H27	-179.6
187	H26	C39	C40	C2	-179.5
188	H26	C39	C40	H27	0.4

GBY-14

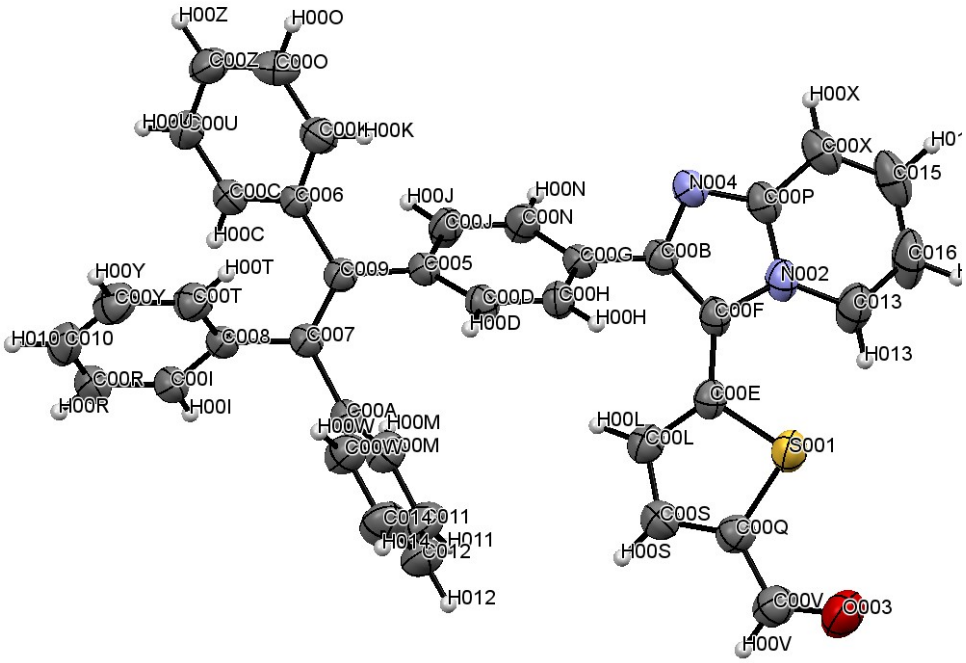

Figure S35. X-Ray crystal structure of **GBY-14** (Ellipsoids with 50% probability).

Table S9. Single crystal data and structure refinement for **GBY-14**.

Identification code	2382114
Empirical formula	$C_{38}H_{26}N_2OS$
Formula weight	558.67
Temperature	296K
Wavelength	0.7107
Crystal system	Triclinic
Space group	P -1
Unit cell dimensions	
a(Å)	9.279 (7)
b(Å)	9.298 (6)

c(Å)	16.663 (13)
α(Å)	90.523 (2)
β(Å)	98.773 (2)
γ(Å)	94.140 (2)
Volume	1416.97 (18)
Z	18
Density (calculated)	1.584
Absorption coefficient	0.757
F(000)	684
Refinement method	SHELXL 2019/3 (Sheldrick, 2015)
Data / restraints / parameters	5352/0/379
Goodness-of-fit on F2	1.027
Final R indices [I>2sigma(I)]	R1 = 0.0675, wR2 = 0.1257
R indices (all data)	R1 = 0.1331, wR2 = 0.1481

$$R_1 = \frac{\sum \| F_0| - |F_c \|}{\sum |F_0|}$$

$$R_w = \sqrt{\frac{\left[\sum \{w(F_0^2 - F_c^2)^2\}\right]}{\left[\sum \{w(F_0^2)^2\}\right]}}$$

Table S10. List Torsion angles [°] for luminogen **GBY-14**

Number	Atom1	Atom2	Atom3	Atom4	Torsion
1	C00Q	S001	C00E	C00F	178.5(2)
2	C00Q	S001	C00E	C00L	0.9(2)
3	C00E	S001	C00Q	C00S	-0.9(2)
4	C00E	S001	C00Q	C00V	174.5(2)

5	C00P	N002	C00F	C00B	-0.0(3)
6	C00P	N002	C00F	C00E	179.3(3)
7	C013	N002	C00F	C00B	-176.7(3)
8	C013	N002	C00F	C00E	2.7(4)
9	C00F	N002	C00P	N004	-0.6(3)
10	C00F	N002	C00P	C00X	179.5(2)
11	C013	N002	C00P	N004	176.5(2)
12	C013	N002	C00P	C00X	-3.3(4)
13	C00F	N002	C013	H013	0.2
14	C00F	N002	C013	C016	-179.9(3)
15	C00P	N002	C013	H013	-176.1
16	C00P	N002	C013	C016	3.8(4)
17	C00P	N004	C00B	C00F	-1.1(3)
18	C00P	N004	C00B	C00G	178.3(2)
19	C00B	N004	C00P	N002	1.1(3)
20	C00B	N004	C00P	C00X	-179.1(3)
21	C00D	C005	C009	C006	137.7(3)
22	C00D	C005	C009	C007	-42.4(4)
23	C00J	C005	C009	C006	-42.1(3)
24	C00J	C005	C009	C007	137.9(3)
25	C009	C005	C00D	H00D	-3.3
26	C009	C005	C00D	C00H	176.7(2)
27	C00J	C005	C00D	H00D	176.5
28	C00J	C005	C00D	C00H	-3.5(4)
29	C009	C005	C00J	H00J	2.7
30	C009	C005	C00J	C00N	-177.3(2)
31	C00D	C005	C00J	H00J	-177

32	C00D	C005	C00J	C00N	2.9(4)
33	C00C	C006	C009	C005	123.8(3)
34	C00C	C006	C009	C007	-56.2(4)
35	C00K	C006	C009	C005	-56.5(3)
36	C00K	C006	C009	C007	123.6(3)
37	C009	C006	C00C	H00C	-3.1
38	C009	C006	C00C	C00U	176.9(2)
39	C00K	C006	C00C	H00C	177.2
40	C00K	C006	C00C	C00U	-2.9(4)
41	C009	C006	C00K	H00K	3
42	C009	C006	C00K	C00O	-177.0(2)
43	C00C	C006	C00K	H00K	-177.2
44	C00C	C006	C00K	C00O	2.8(4)
45	C009	C007	C008	C00I	112.8(3)
46	C009	C007	C008	C00T	-66.7(4)
47	C00A	C007	C008	C00I	-66.5(3)
48	C00A	C007	C008	C00T	114.1(3)
49	C008	C007	C009	C005	179.5(2)
50	C008	C007	C009	C006	-0.5(4)
51	C00A	C007	C009	C005	-1.3(4)
52	C00A	C007	C009	C006	178.6(2)
53	C008	C007	C00A	C00M	123.4(3)
54	C008	C007	C00A	C00W	-56.6(3)
55	C009	C007	C00A	C00M	-55.8(4)
56	C009	C007	C00A	C00W	124.2(3)
57	C007	C008	C00I	H00I	2.9
58	C007	C008	C00I	C00R	-177.1(3)

59	C00T	C008	C00I	H00I	-177.6
60	C00T	C008	C00I	C00R	2.4(4)
61	C007	C008	C00T	H00T	-1.4
62	C007	C008	C00T	C00Y	178.5(3)
63	C00I	C008	C00T	H00T	179.1
64	C00I	C008	C00T	C00Y	-1.0(4)
65	C007	C00A	C00M	H00M	-0.5
66	C007	C00A	C00M	C011	179.5(3)
67	C00W	C00A	C00M	H00M	179.5
68	C00W	C00A	C00M	C011	-0.5(4)
69	C007	C00A	C00W	H00W	1.5
70	C007	C00A	C00W	C014	-178.6(3)
71	C00M	C00A	C00W	H00W	-178.5
72	C00M	C00A	C00W	C014	1.4(4)
73	N004	C00B	C00F	N002	0.7(3)
74	N004	C00B	C00F	C00E	-178.6(3)
75	C00G	C00B	C00F	N002	-178.7(3)
76	C00G	C00B	C00F	C00E	2.1(5)
77	N004	C00B	C00G	C00H	-134.2(3)
78	N004	C00B	C00G	C00N	43.9(4)
79	C00F	C00B	C00G	C00H	45.1(4)
80	C00F	C00B	C00G	C00N	-136.8(3)
81	C006	C00C	C00U	H00U	-179.5
82	C006	C00C	C00U	C00Z	0.5(4)
83	H00C	C00C	C00U	H00U	0.5
84	H00C	C00C	C00U	C00Z	-179.5
85	C005	C00D	C00H	C00G	0.8(4)

86	C005	C00D	C00H	H00H	-179.1
87	H00D	C00D	C00H	C00G	-179.1
88	H00D	C00D	C00H	H00H	0.9
89	S001	C00E	C00F	N002	28.8(4)
90	S001	C00E	C00F	C00B	-152.0(3)
91	C00L	C00E	C00F	N002	-154.0(3)
92	C00L	C00E	C00F	C00B	25.2(5)
93	S001	C00E	C00L	H00L	179.3
94	S001	C00E	C00L	C00S	-0.7(3)
95	C00F	C00E	C00L	H00L	1.8
96	C00F	C00E	C00L	C00S	-178.2(3)
97	C00B	C00G	C00H	C00D	-179.4(3)
98	C00B	C00G	C00H	H00H	0.6
99	C00N	C00G	C00H	C00D	2.5(4)
100	C00N	C00G	C00H	H00H	-177.5
101	C00B	C00G	C00N	C00J	178.8(3)
102	C00B	C00G	C00N	H00N	-1.2
103	C00H	C00G	C00N	C00J	-3.0(4)
104	C00H	C00G	C00N	H00N	177
105	C008	C00I	C00R	H00R	177.9
106	C008	C00I	C00R	C010	-2.2(4)
107	H00I	C00I	C00R	H00R	-2.1
108	H00I	C00I	C00R	C010	177.9
109	C005	C00J	C00N	C00G	0.3(4)
110	C005	C00J	C00N	H00N	-179.7
111	H00J	C00J	C00N	C00G	-179.7
112	H00J	C00J	C00N	H00N	0.3

113	C006	C00K	C00O	H00O	179.7
114	C006	C00K	C00O	C00Z	-0.3(4)
115	H00K	C00K	C00O	H00O	-0.3
116	H00K	C00K	C00O	C00Z	179.7
117	C00E	C00L	C00S	C00Q	0.0(4)
118	C00E	C00L	C00S	H00S	-180
119	H00L	C00L	C00S	C00Q	-180
120	H00L	C00L	C00S	H00S	0
121	C00A	C00M	C011	H011	178.9
122	C00A	C00M	C011	C012	-1.0(4)
123	H00M	C00M	C011	H011	-1.1
124	H00M	C00M	C011	C012	179
125	C00K	C00O	C00Z	C00U	-2.1(4)
126	C00K	C00O	C00Z	H00Z	178
127	H00O	C00O	C00Z	C00U	177.9
128	H00O	C00O	C00Z	H00Z	-2
129	N002	C00P	C00X	H00X	179.8
130	N002	C00P	C00X	C015	-0.2(4)
131	N004	C00P	C00X	H00X	0
132	N004	C00P	C00X	C015	-180.0(3)
133	S001	C00Q	C00S	C00L	0.7(3)
134	S001	C00Q	C00S	H00S	-179.3
135	C00V	C00Q	C00S	C00L	-174.2(3)
136	C00V	C00Q	C00S	H00S	5.8
137	S001	C00Q	C00V	O003	-2.6(4)
138	S001	C00Q	C00V	H00V	177.4
139	C00S	C00Q	C00V	O003	171.8(3)

140	C00S	C00Q	C00V	H00V	-8.2
141	C00I	C00R	C010	C00Y	0.4(4)
142	C00I	C00R	C010	H010	-179.5
143	H00R	C00R	C010	C00Y	-179.6
144	H00R	C00R	C010	H010	0.4
145	C008	C00T	C00Y	H00Y	179.3
146	C008	C00T	C00Y	C010	-0.7(4)
147	H00T	C00T	C00Y	H00Y	-0.8
148	H00T	C00T	C00Y	C010	179.2
149	C00C	C00U	C00Z	C00O	2.0(4)
150	C00C	C00U	C00Z	H00Z	-178.1
151	H00U	C00U	C00Z	C00O	-178
152	H00U	C00U	C00Z	H00Z	2
153	C00A	C00W	C014	C012	-0.8(4)
154	C00A	C00W	C014	H014	179.1
155	H00W	C00W	C014	C012	179.1
156	H00W	C00W	C014	H014	-1
157	C00P	C00X	C015	H015	-176.9
158	C00P	C00X	C015	C016	3.2(5)
159	H00X	C00X	C015	H015	3.1
160	H00X	C00X	C015	C016	-176.8
161	C00T	C00Y	C010	C00R	1.0(4)
162	C00T	C00Y	C010	H010	-179
163	H00Y	C00Y	C010	C00R	-179
164	H00Y	C00Y	C010	H010	1
165	C00M	C011	C012	H012	-178.4
166	C00M	C011	C012	C014	1.6(4)

167	H011	C011	C012	H012	1.7
168	H011	C011	C012	C014	-178.3
169	C011	C012	C014	C00W	-0.7(4)
170	C011	C012	C014	H014	179.4
171	H012	C012	C014	C00W	179.3
172	H012	C012	C014	H014	-0.7
173	N002	C013	C016	C015	-0.8(5)
174	N002	C013	C016	H016	179.1
175	H013	C013	C016	C015	179.2
176	H013	C013	C016	H016	-1
177	C00X	C015	C016	C013	-2.8(5)
178	C00X	C015	C016	H016	177.4
179	H015	C015	C016	C013	177.3
180	H015	C015	C016	H016	-2.5